This is a previous version of the article published in Journal of CO2 Utilization. 2017, 22: 355-373. doi:10.1016/j.jcou.2017.09.019

Multi-objective optimization of combined synthesis gas reforming technologies

Medrano-García, J.D., Ruiz-Femenia, R. and Caballero, J.A.

ABSTRACT: Synthesis gas (syngas) is a mixture of H_2, CO and occasionally CO_2, whose main application is as a building block of chemical compounds. The desired product dictates the syngas characteristics, which are also affected by the employed syngas synthesis technology. In this work, we study the process of producing syngas under desired specifications while consuming CO_2 in the synthesis. We propose a superstructure that includes seven reforming technologies for the syngas production, as well as a variety of auxiliary units to control the final composition of the syngas. Each potential solution is assessed, in terms of the economic and environmental performance, by the Total Annualized Cost (TAC) and the Global Warming Potential (GWP) indicator. As the problem statement involves discrete decision, we use disjunctions to model the system. The resulting MINLP multi-objective problem is solved by the epsilon constraint method. Results show that at low syngas H_2/CO ratios and pressures, dry methane reforming (DMR) is capable of net consuming CO_2. Partial Oxidation (POX) is the technology that exhibits the minimum TAC, although shows the maximum value for the GWP. Synergistic combination of two processes allows reducing the cost and CO_2-equivalent emissions through the pairing of DMR and bi-reforming (BR) and BR with steam methane reforming (SMR). Furthermore, increasing the CO_2 content in the syngas at a fixed (H_2 - CO_2)/(CO + CO_2) ratio proves that TAC and GWP decrease as the CO_2/CO ratio increases.

KEYWORDS: *CO_2 utilization, synthesis gas, methane reforming, superstructure decision making, multi-objective optimization*

ABBREVIATIONS

ASU	Air separation unit
ATR	Auto thermal reforming
BR	Bi-reforming
CR	Combined reforming
DMR	Dry methane reforming

GWP	Global Warming Potential
HI	Heat integration
LCIA	Life Cycle Impact Assessment
POX	Partial oxidation
PSA	Pressure swing adsorption
SMR	Steam methane reforming
STAC	Specific total annualized cost
TAC	Total annualized cost
TR	Tri-reforming
WGS	Water gas shift

NOMENCLATURE

Indices

i	syngas processes: SMR, POX, ATR, CR, DMR, BR, TR
j	components: methane, steam/water, O_2, CO_2, CO, H_2
k	syngas process units: compressor, exchanger/heater/cooler, reformer reactor
m	post processing units: absorber1, WGS reactor, bypass1, flash, PSA, compressor, bypass2, absorber2, bypass3
u	utilities: natural gas, cooling water, power

Parameters

AF	annualization factor
B_k^1	bare module parameter 1 of unit k
B_k^2	bare module parameter 2 of unit k
c_{ik}^f	fixed cost of unit k in process i [$]

53	c_{ik}^{v}	variable cost of unit k in process i [$/capacity units]
54	c_{f}^{m}	fixed cost of auxiliary unit m [$]
55	c_{v}^{m}	variable cost of auxiliary unit m [$/capacity units]
56	F_{ik}^{P}	pressure factor of unit k
57	F_{k}^{M}	material factor of unit k
58	$F_{\max}$	upper flowrate limit [kmol/h]
59	IR	fractional interest rate per year
60	K_{eq}	equilibrium constant for WGS reaction
61	M	stoichiometric syngas number
62	nsp	maximum number of existing syngas processes
63	P_{i}	operating pressure in process i [bar]
64	$P_{\max}$	upper pressure limit [bar]
65	P_{syngas}	target pressure of the final syngas [bar]
66	T_{feed}	temperature of the stream fed to a compressor [K]
67	t_{h}	operating hours per year [h]
68	T_{i}	temperature of the stream leaving process i fed its compressor [K]
69	V_{abs1}	volume of absorber column 1
70	V_{abs2}	volume of absorber column 2
71		
72	β_{iu}	cost of utility u in process i [$/kmol methane fed]
73	χ_{ij}	conversion for component j in process i [kmol j / kmol methane fed]
74	δ_{j}	cost of raw material j [$/kmol]
75	ε	multiobjective optimization epsilon parameter
76	$\underline{\varepsilon}$	lower bound of multiobjective optimization epsilon parameter

$\overline{\varepsilon}$ upper bound of multiobjective optimization epsilon parameter

ϕ_j GWP associated to raw material j [kg CO_2-eq/kmol *j*]

φ_{iu} GWP associated to utility u in process i [kg CO_2-eq/kmol methane fed]

Variables

cap_i capital cost of process i [$]

cap_m capital cost of auxiliary unit m [$]

$cost_i$ total cost of process i [$]

$cost_m$ total cost of auxiliary unit m [$]

$emission_i$ total GWP of process i [kg CO_2-eq]

$emission_m$ total GWP of auxiliary unit m [kg CO_2-eq]

F_{abs} absorbed CO_2 flowrate [kmol/h]

F_{H_2} hydrogen flowrate separated in the PSA unit [kmol/h]

F_{ij} outlet molar flowrate of component j in process i [kmol/h]

F_{ij}^0 inlet molar flowrate of component j in process i [kmol/h]

$F_j^{recycle}$ component j recycled flowrate to the exist of the syngas processes [kmol/h]

$F_j^{m,in}$ inlet flowrate of component j to unit m [kmol/h]

$F_j^{m,out}$ outlet flowrate of component j to unit m [kmol/h]

op_i operating cost of process i [$]

op_m operating cost of auxiliary unit m [$]

P_i^{out} outlet pressure of compressor i [bar]

P_{mix} pressure after the stream convergence before the WGS/absorber selection [bar]

$power_i^{comp}$ electricity consumption of compressor after process i [kW]

$power_m$ electricity consumption of auxiliary unit m [kW]

raw_i	raw material cost of process of process i [$]
y_i	binary variable associated to the existence of process i
y_i^{comp}	binary variable associated to the existence the compressor after process i
y_m	binary variable associated to the existence of auxiliary unit m
Y_i	Boolean variable associated to the existence of process i
Y_i^{comp}	Boolean variable associated to the existence the compressor after process i
Y_m	Boolean variable associated to the existence of auxiliary unit m
ΔP_i	increase in pressure achieved in compressor i [bar]

1. Introduction

Carbon dioxide has been a matter of concern for the last decades. Its continuous and increasing emission, which is almost guaranteed in any industrial process involving a chemical combustion, must be controlled due to CO_2 being one of the main greenhouse agents originating global warming [1]. In view of this situation, the imperious need to reduce these emissions has been a fact for a long time. The use of low carbon content fuels, improving energy efficiency, the development of new and cleaner technologies or the increasing implementation of renewable energy sources are, amongst other, different approaches made to palliate the problem [2].

Synthesis gas (syngas) is a mixture of gases, mainly formed by hydrogen and carbon monoxide, although carbon dioxide might be also present depending on the application. Syngas can be produced by gasification or reforming of virtually any hydrocarbon source [3] and a reforming agent, like steam, oxygen, carbon dioxide or mixtures of them. Using methane as the carbon source and depending on the reforming agent or mixture of them used, syngas reforming technologies are divided into (Figure 1): steam methane reforming (SMR), partial oxidation (POX), auto thermal reforming (ATR), combined reforming (CR), dry methane reforming (DMR), bi-reforming (BR), tri-reforming (TR). ATR of natural gas was first introduced by Haldor-Topsoe [4, 5] and is also the preferred reforming technology of Sasol [6, 7], Air Liquid [8], John Matthey Process Technologies [9] and BP [10] when reforming methane. On the other hand,

POX is used by Linde, one of the major contractors of this technology world-wide, which operates the largest plant with natural gas charge (200 00 Nm^3/h of syngas) [11, 12]. CR is also used as an alternative by Haldor-Topsoe [5] and Linde [11] among others, although at a lesser extent than the previous two technologies. SMR is the preferred technology when hydrogen content syngas is required or hydrogen is desired as a byproduct [13].

The "quality" of the syngas changes in each process. This property can be measured with the stoichiometric number also known as *M*, which general formula is:

$$M = \frac{F_{H_2} - F_{CO_2}}{F_{CO} + F_{CO_2}} \quad (1)$$

where F_i is the molar flow (or partial pressure, concentration, etc.) in the syngas. The desired value of *M* is not set in stone, since depending on the application it can range from almost zero (mainly CO when there is no CO_2) to high values in order to get pure hydrogen (Figure 2).

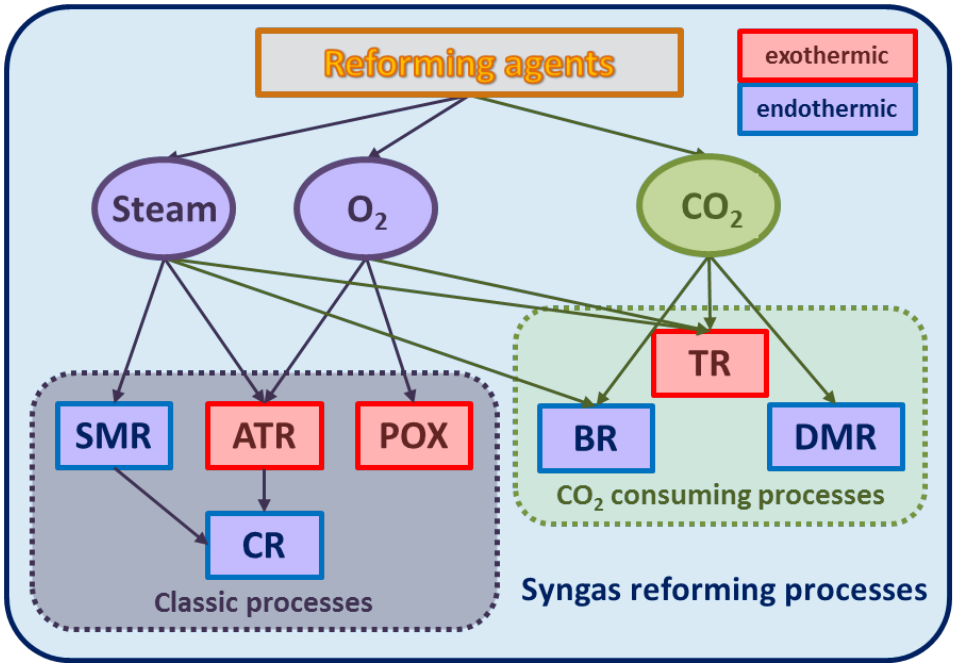

Figure 1. Syngas reforming technologies sorted by reforming agents employed.

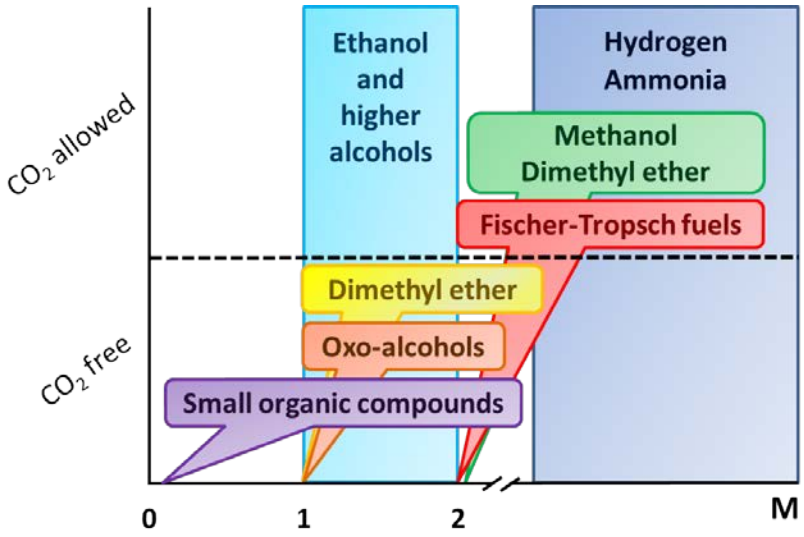

Figure 2. Downstream applications of syngas for chemical production as a function of the stoichiometric number M = $(H_2\text{-}CO_2)/(CO+CO_2)$. CO_2 allowance in a process is optional, and in the case of hydrogen and ammonia CO_2 present is not consumed.

Reforming technologies are cost intensive due to the high temperatures required to carry out the reactions (see section 2). In addition, the massive use of fuel significantly increases emissions while operating the plant. However, these aspects led to the development of the combined reforming technology [14], which uses SMR and ATR in a single process. This combination allows not only gaining more control over the H_2/CO ratio but also using the exothermicity of ATR to partially fuel the SMR reactor. Several authors have studied other combinations of these technologies. Lim et al. [15] proposed a combination of SMR and DMR in which the latter used the CO_2 produced in the former to increase the syngas production, successfully mitigating both cost and emissions. Farniaei et al. thermally coupled the exothermic TR with SMR and DR [16, 17] in concentric reactors, producing two different composition syngas flows (mixable to achieve a specific ratio) while reducing the energy consumption.

In this work, we propose a superstructure to manufacture syngas with a specific composition. This superstructure includes classic (i.e., non-CO_2 consuming) and CO_2 consuming reforming processes as well as a posttreatment section in which the syngas composition is further adjusted to the specified ratio. A number of composition and pressure combinations are studied to fulfill a range of syngas specifications. Multi-objective optimizations are carried out using Global Warming Potential (GWP) and the Specific Total Annualized Cost (STAC) as the objectives for just one and combination of two syngas processes. Results show that the different Pareto curves are greatly affected by the final syngas composition and pressure.

2. Methods and models

2.1. Syngas process structure

Each syngas process has been designed following the scheme shown in Figure 3. An initial feedstock at 25 °C and 1 bar, composed by methane or methane and a selected reforming agent or mixture of them, enters a compression stage and is pressurized up to the working pressure. Then, steam (as raw material) is added if necessary (Table 1 shows the available types of steam). The mixture is then preheated at the reformer furnace temperature and enters the reactor. Syngas leaving the reformer is finally cooled to 250 °C and sent to the composition adjustment stage.

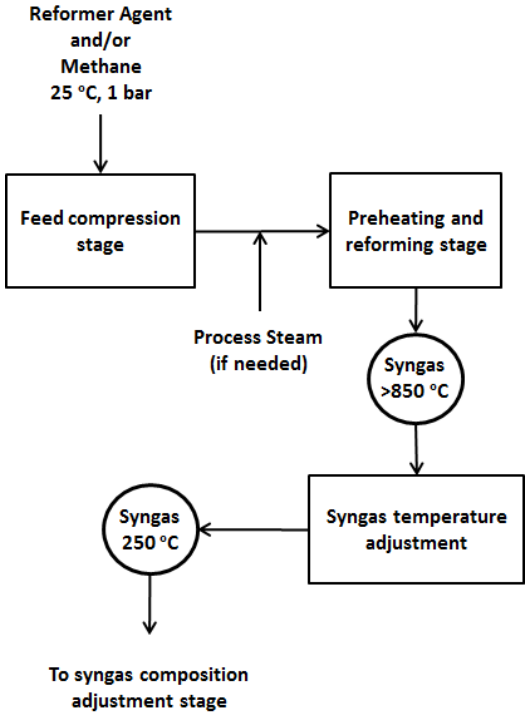

Figure 3. General syngas process flow diagram.

Table 1. Pressure, temperature and for each type of steam [18].

	Low pressure	Medium pressure	High pressure
Pressure [barg]	5	10	41
Temperature [°C]	160	184	254
Cost [$/1000kg]	29.29	29.59	29.97

Coolers use liquid water at 30 °C leaving the exchangers at 40 °C [18]. Preheaters and reforming reactors, when needed, are fueled by natural gas combustion. It has been proved that most of the syngas processes lead to a conversion of methane near the equilibrium [16, 17, 19-25]. Consequently, and for the sake of simplicity, we carry out the simulations in Aspen HYSYS v8.4 using Gibbs equilibrium— along with the required operation units— to pre-calculate the conversions and the utility consumption for each technology. Optimal temperatures, pressures and feed ratios have been chosen not only to favor conversion but also to avoid real problems like soot formation or quick deactivation of catalysts. These operating conditions can be found in Table 2. Additional data, such as prices and Life Cycle Impact Assessment (LCIA) values (Global Warming Potential (GWP) for 100 years time horizon) of the raw materials are shown in Table 3. LCIA data were retrieved from the Ecoinvent environmental database [26]. In addition, Table 4 provides the prices and LCIA values for the utilities employed.

Table 2. Reforming agent/methane molar ratio in the feed stream and operating conditions for each syngas process [16, 17, 19-25].

	SMR	**POX**	**ATR**	**CR**	**DMR**	**BR**	**TR**
H_2O/CH_4	3	-	1.43	2.5	-	1.6	2.46
O_2/CH_4	-	0.7	0.6	0.19	-	-	0.47
CO_2/CH_4	-	-	-	-	1	0.8	1.3
Temperature [°C]	900	800	750	850	850	850	827
Pressure [bar]	20	30	25	25	1	7	20

Due to the high temperatures required to perform the reforming reactions, heat integration (HI) has been implemented in order to save energy and reduce the cost and emissions related to them. The SYNHEAT [27] model within GAMS has been used in order to calculate the resulting exchanger areas. The results of the HI analysis as well as a comparison with the base processes are shown in Table 5. Syngas processes before and after heat integration can be found in Appendix A.

Table 3. Prices and LCIA values for the raw materials [28, 29].

Feed	**Source**	**Price [$/kg]**	**GWP [kg CO_2-eq/kg]**
Methane	Global market (96% volume)	0.2441	0.9103

Steam	Global market (chemical industry)	(see Table 1)	0.18302
Oxygen	Cryogenic air separation unit	0.155	0.67043
Carbon dioxide	Amine absorption	0.04306	1

Table 4. Utility prices and LCIA values [18, 28].

Utility	**Source**	**Price [$/kWh]**	**GWP [kg CO_2-eq/kWh]**
Natural gas	Heat production at industrial furnace	0.0424	0.2122
Cooling water	Process cooling water (30°C to 40 or 45°C)	0.0013	-
Electricity	High voltage	0.1086	0.61365

Table 5. Cooling services (CS) and heating services (HS) required before and after performing heat integration (HI) (units in kW per kmol/h of syngas).

Process	**SMR**	**POX**	**ATR**	**CR**	**DR**	**BR**	**TR**
Base CS	7.02	9.56	10.39	7.80	5.282	5.763	7.27
CS after HI	1.33	6.67	5.24	0.40	0	1.48	0.52
% reduced	81	30	50	95	100	74	99
Base HS	19.94	4.49	7.42	17.26	23.88	17.37	9.49
HS after HI	9.47	0	0	8.02	19.98	11.80	0.64
% reduced	52	100	100	53	16	32	90

2.2. Auxiliary units

All the alternatives of interest for the production of syngas are embedded in the superstructure proposed in Figure 4.

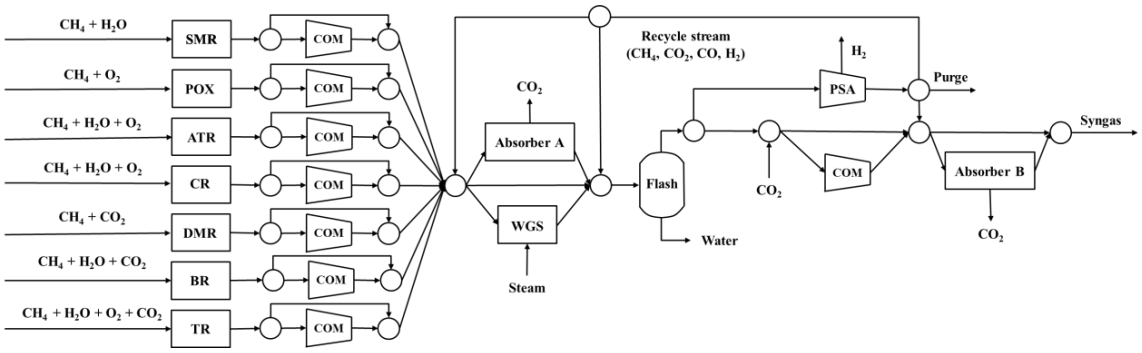

Figure 4.Proposed superstructure embedding the syngas process alternatives and specification adjustment units.

Auxiliary units are included after the main syngas process in order to adjust the syngas composition and pressure. Syngas needed for product synthesis not only requires different compositions but also pressures. For this reason, the syngas exiting the synthesis stage can be pressurized depending on the demanding pressure. Regarding the composition, a phase separator, used to remove water from syngas, is assumed to accomplish perfect separation. Hydrogen separated with the pressure swing adsorption (PSA) unit comprises 90 % of the total inlet with a 99 % of purity. More information and its capital cost model can be found in [30-32]. Absorbers work at 40 °C and use 48 % wt DGA with 96 % CO_2 recovery with an operating cost of 43.06 \$/ton CO_2 absorbed [29]. A water gas shift (WGS) reactor is operated at 250 °C and considered capable of reaching the equilibrium, which is calculated following the equilibrium constant (K_{eq}) [33]:

$$K_{eq} = \exp\left(\frac{4577.8}{T} - 4.33\right) \tag{2}$$

2.3. Mathematical modelling of the superstructure

As can be seen in the superstructure (Figure 4), the initial feedstock enters a selected syngas process amongst the possible options, and exits the process as syngas. Since ratios methane/reforming agents, temperatures and pressures are known for each alternative (Table 2), each process can be simulated in ASPEN HYSYS v8.4 to obtain conversions and energy requirements. Conversion for component j in process i , χ_{ij} , is computed using this relation:

$$F_{ij} = \chi_{ij} F^{0}_{i\,methane} \qquad \forall i, j \tag{3}$$

where F_{ij} is the molar flowrate in the outlet stream of the process and $F^{0}_{i\,methane}$ is the molar flowrate of methane fed to the process. The values of χ_{ij} along with other calculated

parameters employed in the model are presented in Appendix B. The total cost of a syngas process is calculated as:

$$cost_i = raw_i + cap_i + op_i \qquad \forall i \tag{4}$$

The variable $cost_i$ indicates the total cost in \$ of process i, and raw_i, cap_i and op_i are the raw material, capital and operating costs in \$ of process i, respectively, which are individually defined as:

$$raw_i = \sum_j \delta_j F_{ij}^0 t_h \qquad \forall i \tag{5}$$

$$cap_i = \sum_k \left(c_{ik}^f + c_{ik}^v F_{i\,methane}^0 \right) \left(B_k^1 + B_k^2 F_k^M F_{ik}^P \right) \qquad \forall i \tag{6}$$

$$op_i = \sum_u \beta_{iu} F_{i\,methane}^0 t_h \qquad \forall i \tag{7}$$

where δ_j, is the cost in \$/kmol of raw material j, F_{ij}^0 is the initial molar flow of species j in process i, t_h is the annual operating time (8000 h), c_{ik}^f (\$) and c_{ik}^v (\$/kmol of raw methane) are a fixed and variable cost parameters of unit k (compressor, exchanger, reactor) in process i. F_k^M and F_{ik}^P are the material and pressure factors of unit k, B_k^1 and B_k^2 are the bare module parameters of unit k and β_{iu} (\$/kmol of fresh methane) is the product of the energetic demand in kWh per kmol of raw methane entering the process of utility u (natural gas, cooling water, power) and the cost of said utilities (\$/kWh). To estimate the capital cost, the required nonlinear models of Turton et al. [18] were linearized to improve the quality of the optimization (Appendix B).

The emissions in kilograms of carbon dioxide equivalent (kg CO_2-eq) per hour associated to the syngas process i ($emission_i$) are calculated with the expression:

$$emission_i = \left(\sum_u \varphi_{iu} F_{i\,methane}^0 + \sum_j \phi_j F_{ij}^0 - F_{iCO_2}^0 \right) t_h \qquad \forall i \tag{8}$$

where the parameter φ_{iu} represents kg of CO_2-eq emitted of utility u per kmol of methane fed to process i (Appendix B), and ϕ_j the kg of CO_2-eq emitted per kmol of raw material j (Table 3).

To handle the conditional existence or non-existence of a particular syngas process i, we write the following disjunction:

$$\begin{bmatrix} Y_i \\ F_{ij} = \chi_{ij} F^0_{imethane} \\ cap_i = \sum_k \left(c^f_{ik} + c^v_{ik} F^0_{imethane} \right) \left(B^1_k + B^2_k F^M_k F^P_k \right) \quad \forall i \\ 0 \le \sum_j F_{ij} \le F_{\max} \\ 0 \le \sum_j F^0_{ij} \le F_{\max} \end{bmatrix} \veebar \begin{bmatrix} \neg Y_i \\ F^0_{ij} = 0 \\ F_{ij} = 0 \\ cap_i = 0 \end{bmatrix} \quad \forall i \tag{9}$$

where Y_i is a Boolean variable related to the existence of syngas process i. If the Boolean variable is true then the process has flows, costs and emissions associated to it, otherwise, all the variables associated with the process are set to zero. This disjunction can be reformulated into a set of algebraic equations using a binary variable (y_i) which adopts the values 1 or 0 if the corresponding Boolean variable is true or false, respectively. Since all the equations enclosed in the disjunction are linear, we apply the Hull reformulation [34]. The reformulation is as follows:

$$F_{ij} = \chi_{ij} F^0_{imethane} \tag{10}$$

$$cap_i = \sum_k \left(y_i c^f_{ik} + c^v_{ik} F^0_{imethane} \right) \left(B^1_k + B^2_k F^M_k F^P_k \right) \qquad \forall i \tag{11}$$

$$0 \le F_{ij} \le y_i F_{\max} \qquad \forall i, j \tag{12}$$

$$0 \le F^0_{ij} \le y_i F_{\max} \qquad \forall i, j \tag{13}$$

Moreover, to limit the number of selected syngas processes, the next equation must be included in the model:

$$\sum_i y_i \le nsp \tag{14}$$

where nsp is the number of selected syngas processes. After the syngas is synthesized, the option of changing the pressure is given. A compressor per process may or may not exist:

279
$$\begin{bmatrix} Y_i^{comp} \\ cost_i^{comp} = c_f^{comp} + c_v^{comp}\, power_i^{comp} \\ 0 \le \sum_j F_{ij}^{comp} \le F_{\max} \\ 0 \le \Delta P_i \le P_{\max} \end{bmatrix} \veebar \begin{bmatrix} \neg Y_i^{comp} \\ cost_i^{comp} = 0 \\ F_{ij}^{comp} = 0 \\ \Delta P_i = 0 \end{bmatrix} \qquad \forall i \tag{15}$$

280 where F_{ij}^{comp} is the component *j* molar flow coming from syngas process *i* that enters and exits
281 its respective compressor, $P_{\max}$ is the upper limit that the pressure can reach (30 bar), P_i is
282 the pressure at which each syngas process i operates (bar), ΔP_i is the increase of pressure
283 gained in the compressor (bar) with an energy consumption ($power_i^{comp}$) in kW calculated as:

284

285
$$power_i^{comp} = \left(\frac{\gamma}{\gamma - 1}\right) \eta^{-1} R_g T_i \sum_j F_{ij}^{comp} \left[\left(\frac{P_i^{out}}{P_i} \right)^{\left(\frac{\gamma}{\gamma-1}\right)} - 1 \right] \tag{16}$$

286 where γ is the heat capacity ratio assumed constant at 1.5, η is the compressor efficiency
287 fixed at 0.8 and R_g and T_i are the universal gas constant and the inlet stream temperature
288 respectively and P_i^{out} is the outlet compressor pressure (bar). Applying the Hull reformulation
289 to disjunction **¡Error! No se encuentra el origen de la referencia.** results in:

290
$$cost_i^{comp} = c_f^{comp} y_i^{comp} + c_v^{comp}\, power_i^{comp} \tag{17}$$

291
$$0 \le \sum_j F_{ij}^{comp} \le F_{\max} y_i^{comp} \tag{18}$$

292
$$0 \le \Delta P_i \le P_{\max} y_i^{comp} \tag{19}$$

293 while the outlet pressure of the potential compression stage i is calculated as:

294
$$P_i^{out} = P_i + \Delta P_i \tag{20}$$

295 where y_i^{comp} is a binary variable associated to the existence of the compressor. In addition, if a
296 compressor i exists then its associated process i must be selected, leading to the Boolean
297 relation:

298
$$Y_i^{comp} \Rightarrow Y_i \tag{21}$$

299 which translates into:

300 $$y_i - y_i^{comp} \geq 0 \tag{22}$$

301 When more than one syngas process exists, the mixture of both syngas streams will result in a
302 new stream with the lowest pressure of the two (P_{mix}). Since the selected processes are
303 unknown beforehand, the outlet pressures of the compression stage for all technologies are
304 considered in the minimum operator:

305 $$P_{mix} = \min(P_1^{out}, P_2^{out}, ..., P_i^{out}) \tag{23}$$

306 Pressure is a decision variable with a relevant contribution both in cost and emission: the
307 higher the target pressure is, the higher the cost and emission associated are to reach it.
308 Therefore, when mixing the two streams, both objective functions will tend to maximize the
309 pressure if it is let free to reduce compressor power. Since the min operator introduces a
310 discontinuity in the model, we compute P_{mix} by replacing Eq.(23) with the following set of
311 constraints, which are suited for the optimization problem:

312 $$P_{mix} \leq P_i^{out} + P_{\max}(1 - y_i) \qquad \forall i \tag{24}$$

313 where P_{mix} is the final pressure after the stream mixture. According to Eq.(24), the minimum
314 pressure of the mixture and thus, the most restrictive upper limit of P_{mix} will become the final
315 value. After the mixture, the product syngas splits into at most three branches (Figure 4). Since
316 all the streams reaching this point are at the same temperature (Figure 3), this node is
317 modeled by a total (Eq.(25)) and component molar balances (Eqs.(26)-(28)) forcing that the
318 concentration for each component in each stream leaving the node is the same than the
319 average concentration of that component calculated from the two inlet streams to the node:

320 $$\sum_i F_{ij} + F_j^{recycle} = F_j^{WGS,in} + F_j^{bp1,in} + F_j^{abs1,in} \qquad \forall i, j \tag{25}$$

321 $$F_j^{WGS,in}\left(\sum_i F_{ij} + F_j^{recycle}\right) = \left(F_{ij} + F_j^{recycle}\right)\sum_j F_j^{WGS,in} \qquad \forall j \tag{26}$$

322 $$F_j^{abs1,in}\left(\sum_i F_{ij} + F_j^{recycle}\right) = \left(F_{ij} + F_j^{recycle}\right)\sum_j F_j^{abs1,in} \qquad \forall j \tag{27}$$

$$F_j^{bp1}\left(\sum_i F_{ij} + F_j^{recycle}\right) = \left(F_{ij} + F_j^{recycle}\right)\sum_j F_j^{bp1} \qquad \forall j \tag{28}$$

where $F_j^{recycle}$ is the molar flow recycled from the PSA unit and $F_j^{WGS,in}$, $F_j^{abs1,in}$, $F_j^{bp1,in}$ are the inlet molar flows of the WGS reactor, first absorber and first bypass, respectively. These nonlinear component molar balances are unavoidable in order to correctly define the splitter nodes, as their absence would result in the split streams potentially having different compositions. Since a structural decision must be taken from these three options, we add the following disjunctions to the model. For the absorber, the disjunction results in:

$$\begin{bmatrix} Y_{abs1} \\ cost_{abs1} = cap_{abs1} + 1.89F_{abs1}t_h \\ 0 \le \sum_j F_j^{abs1,in} \le F_{\max} \\ 0 \le \sum_j F_j^{abs1,out} \le F_{\max} \\ 0 \le F_{abs1} \le F_{\max} \end{bmatrix} \veebar \begin{bmatrix} \neg Y_{abs1} \\ F_j^{abs1,in} = 0 \\ F_j^{abs1,out} = 0 \\ F_{abs1} = 0 \\ cost_{abs1} = 0 \end{bmatrix} \tag{29}$$

where $F_j^{abs1,out}$ refers to component *j* molar flowrate exiting the absorber in kmol/h, F_{abs1} is the CO_2 molar flow absorbed in kmol/h, $cost_{abs1}$ is the total cost of the absorber in \$/h and cap_{abs1} is the capital cost of the absorber in \$/h and has an equivalent form as Eq. (11). The absorber mass balances in conjunction with the expressions resulting from applying the Hull reformulation to Eq.(29) are used to model the absorber:

$$F_j^{abs1,out} = F_j^{abs1,in} \quad \forall j \setminus \{CO_2\} \tag{30}$$

$$F_{CO_2}^{abs1,out} = F_{CO_2}^{abs1,in} - F_{abs1} \tag{31}$$

$$F_{abs1} = 0.96F_{CO_2}^{abs1,in} \tag{32}$$

$$cost_{abs1} = cap_{abs1} + 1.89F_{abs1}t_h \tag{33}$$

$$cap_{ab1} = \left(y_{abs1}c_{abs1}^f + c_{abs1}^v V_{abs1}\right)\left(B_{abs1}^1 + B_{abs1}^2 F_{abs1}^M F_{abs1}^P\right) \tag{34}$$

$$0 \le \sum_j F_j^{abs1,in} \le F_{\max} y_{abs1} \tag{35}$$

$$0 \le \sum_j F_j^{abs1,out} \le F_{\max} y_{abs1} \tag{36}$$

$$0 \le F_{abs1} \le F_{\max} y_{abs1} \tag{37}$$

where y_{abs1} is the binary variable associated to the selection of absorber column 1 and V_{abs1} is the volume of the absorber column 1 assumed as 100 m^3.

For the water gas shift reactor, in order to maintain the model as simple as possible, we used the equilibrium constant (Eq.(2)) at 250 °C along with Eq.(38):

$$K_{eq} = \frac{F_{H_2}^{WGS,out} F_{CO_2}^{WGS,out}}{F_{CO}^{WGS,out} F_{H_2O}^{WGS,out}} \tag{38}$$

where $F_j^{WGS,out}$ represents the molar flow of component *j* exiting the WGS reactor in kmol/h. Volume of the reactor is fixed at 100 m^3 for capital cost calculation. The bypass is not required to be included in a disjunction since its existence is not tied to a cost, so only a simple mass balance indicating that the outlet flow ($F_j^{bp1,out}$) is the same as the inlet flow ($F_j^{bp1,in}$) is needed:

$$F_j^{bp1,out} = F_j^{bp1,in} \qquad \forall j \tag{39}$$

The absorber, bypass and reactor can be used simultaneously and at least one of them must exist, this is represented by the logic relation:

$$\sum_m y_m \ge 1 \qquad m \in \{abs1, bp1, WGS\} \tag{40}$$

The flash separator removes water in a simple material balance, letting the rest of the components pass through it. Since water is present in all the alternatives, the flash separator is a mandatory unit and a disjunction is not required to model it. After drying the syngas, two choices are again encountered: a PSA unit to purify H_2 and a branch which divides into a second bypass and a compressor. Again, the splitter after the flash unit is modeled using equivalent expressions to Eqs.(25)-(28). The PSA unit requires 30 bar to carry out the adsorption of hydrogen, while it is desorbed at 1 bar. The low hydrogen content syngas is considered to maintain 30 bar at the exit of the PSA. Then, this flow can return at the absorber/WGS node, continue the superstructure path and/or be purged to avoid the

methane build up in the superstructure. The pure hydrogen flow is not taken into account in the cost calculation. The PSA unit associated disjunction is presented in Eq.(41):

$$\begin{bmatrix} Y_{PSA} \\ cost_{PSA} = cap_{PSA} + op_{PSA} \\ 0 \le \sum_j F_j^{PSA,in} \le F_{\max} \\ 0 \le \sum_j F_j^{PSA,out} \le F_{\max} \\ 0 \le F_{H_2} \le F_{\max} \end{bmatrix} \veebar \begin{bmatrix} \neg Y_{PSA} \\ F_j^{PSA,in} = 0 \\ F_j^{PSA,out} = 0 \\ F_{H_2} = 0 \\ cost_{PSA} = 0 \end{bmatrix} \tag{41}$$

where F_{H_2} is the pure hydrogen flow in kmol/h separated in the PSA. Applying the Hull reformulation and adding the mass balances lead to:

$$F_j^{PSA,out} = F_j^{PSA,in} \quad \forall j \setminus \{H_2\} \tag{42}$$

$$F_{H_2}^{PSA,out} = F_{H_2}^{PSA,in} - F_{H_2} \tag{43}$$

$$F_{H_2}^{PSA,out} = 0.1 F_{H_2}^{PSA,in} \tag{44}$$

$$cost_{PSA} = cap_{PSA} + op_{PSA} \tag{45}$$

$$cap_{PSA} = y_{PSA} c_f^{PSA} + c_v^{PSA} F_{H_2}^{PSA,in} \tag{46}$$

$$op_{PSA} = 0.1086\, power_{PSA} t_h \tag{47}$$

$$power_{PSA} = \left(\frac{\gamma}{\gamma - 1} \right) \eta^{-1} R_g T_{feed} \sum_j F_j^{PSA,in} \left[\left(\frac{P_h}{P_{out}} \right)^{\left(\frac{\gamma}{\gamma - 1} \right)} - 1 \right] \tag{48}$$

$$0 \le \sum_j F_j^{PSA,out} \le F_{\max} y_{PSA} \tag{49}$$

$$0 \le \sum_j F_j^{PSA,in} \le F_{\max} y_{PSA} \tag{50}$$

$$0 \le F_{H_2} \le F_{\max} y_{PSA} \tag{51}$$

where T_{feed} is the inlet molar flow temperature fixed at 40 °C and P_h and P_l are the outlet (30 bar) and inlet pressures.

The branch parallel to the PSA unit, which divides into a bypass and a compressor, can be selected simultaneously with the PSA unit. However, the bypass and the compressor cannot exist at the same time. In addition, an optional CO_2 stream (F_{CO_2}) can be mixed before the compressor/bypass division if it is required to adjust the composition. The disjunction for the existence of the compressor can be seen in Eq.(52):

$$\begin{bmatrix} Y_{comp} \\ cost_{comp} = cap_{comp} + op_{comp} \\ 0 \le \sum_j F_j^{comp,out} \le F_{\max} \\ 0 \le \sum_j F_j^{comp,in} \le F_{\max} \end{bmatrix} \underline{\vee} \begin{bmatrix} \neg Y_{comp} \\ F_j^{comp,in} = 0 \\ F_j^{comp,out} = 0 \\ cost_{comp} = 0 \end{bmatrix} \quad \forall j \tag{52}$$

reformulating and including the rest of the model equations:

$$F_j^{comp,out} = F_j^{comp,in} \quad \forall j \tag{53}$$

$$cost_{comp} = cap_{comp} + op_{comp} \tag{54}$$

$$cap_{comp} = y_{comp} c_f^{comp} + c_v^{comp} power_{comp} \tag{55}$$

$$op_{comp} = 0.1086\, power_{comp} t_h \tag{56}$$

$$power_{comp} = \left(\frac{\gamma}{\gamma - 1} \right) \eta^{-1} R_g T_{feed} \sum_j F_j^{comp,in} \left[\left(\frac{P_{syngas}}{P_{comp}} \right)^{\left(\frac{\gamma}{\gamma - 1} \right)} - 1 \right] \tag{57}$$

$$0 \le \sum_j F_j^{comp,out} \le F_{\max} y_{comp} \tag{58}$$

$$0 \le \sum_j F_j^{comp,in} \le F_{\max} y_{comp} \tag{59}$$

where P_{comp} is pressure before the compressor. Since P_{syngas} is a fixed value for each optimization, the final pressure could be obtained even if the compressor is not chosen, for this reason we add the next restriction:

$$P_{comp} \ge P_{syngas} \left(1 - y_{comp} \right) \tag{60}$$

When P_{comp} is greater or equal than P_{syngas} the compressor is not needed and pressure has to be reduced (or unaltered) to fulfill the pressure constraint. However, if P_{comp} is lower than P_{syngas}, the compressor has to exist so Eq.(60) is satisfied.

The second bypass of the superstructure, parallel to the final compressor, is modelled as the previous one:

$$F_j^{bp2,out} = F_j^{bp2,in} \qquad \forall j \tag{61}$$

The exclusive existence of the compressor or the bypass is accounted as:

$$\sum_m y_m = 1 \qquad m \in \{comp, bp2\} \tag{62}$$

On the final part of the superstructure, a second absorber (abs2) along with another bypass (bp3) are added. This additional absorber serves as the last CO_2 removal tool. In case of not needing an additional CO_2 removal stage, or if just a fraction of the CO_2 needs to be extracted, the bypass is selected. The absorber column 2 follows the same model as the first absorber (Eqs.(30)-(37)) while the bypass is defined as the other ones (Eq.(39) and Eq.(61)). Both follow the 'at least one' relation previously described:

$$\sum_m y_m \geq 1 \qquad m \in \{abs2, bp3\} \tag{63}$$

After this last alternative, the final syngas molar flow with the desired composition is obtained. The Total Annualized Cost (TAC) of the system is calculated using Eq.(64):

$$TAC = \left(\sum_i cap_i + \sum_m cap_m \right) AF + \sum_i \left(op_i + raw_i \right) + \sum_m op_m \tag{64}$$

$$AF = \frac{IR\left(IR+1\right)^{years}}{\left(IR+1\right)^{years} - 1} \tag{65}$$

where AF is the annualization factor, the horizon time is 10 years and the interest rate (IR) is set to 0.8.

Global Warming Potential (GWP) is estimated as the sum of the net emissions (direct and indirect) of the syngas reforming processes and auxiliary units:

425 $$GWP = \sum_i emission_i + \sum_m emission_m - F_{CO_2} \quad (66)$$

426 For both TAC and GWP calculations, a total of 8000 operating hours a year are taken into
427 account.

428 *2.4. Multiobjective optimization*

429 The overall bi-MINLP formulation can be finally expressed in compact form as follows:

430 $$\begin{aligned} &\min_{x,y} \{TAC(x,y); -GWP(x,y)\} \\ &s.t. \qquad constraints \end{aligned} \quad (67)$$

431 where x and y generically denotes continuous variables associated with structural decisions.
432 The solution to this problem is given by a set of Pareto alternatives representing the optimal
433 trade-off between the two objectives. In this work, these Pareto solutions are determined via
434 the ε-constraint method [35] which solves a set of instances of the following single-objective
435 problem M1 for different values of the auxiliary parameter ε:

436 $$(M1) \qquad \begin{aligned} &\min_{x,y} \{TAC\} \\ &s.t. \quad constraints \\ &\quad GWP \le \varepsilon \\ &\quad \underline{\varepsilon} \le \varepsilon \le \overline{\varepsilon} \end{aligned} \quad (68)$$

437 where the lower and upper limits of epsilon are obtained from the optimization of each
438 separate scalar objective. We obtain the highest value for the GWP (that is $\overline{\varepsilon}$) by solving the
439 following problem (M1a):

440 $$(M1a) \qquad \begin{aligned} &(\overline{x}, \overline{y}) = \arg\min_{x,y} \{TAC\} \\ &s.t. \quad \text{constraints} \end{aligned} \quad (69)$$

441 From the solution of problem (M1a), we calculate $\overline{\varepsilon} = GWP(\overline{x}, \overline{y})$. The best environmental
442 performance is obtained regardless of the economic aspect. Hence we obtain the lowest value
443 for the GWP (that is $\underline{\varepsilon}$) as the optimum value of the objective function for the next mono-
444 objective problem:

445 $$(M1b) \qquad \begin{aligned} &\underline{\varepsilon} = \min_{x,y} \{GWP\} \\ &s.t. \quad \text{constraints} \end{aligned} \quad (70)$$

446 $$(M1b) \qquad \begin{aligned} \underline{\varepsilon} &= \min_{x,y} \{GWP\} \\ s.t. \quad & \text{constraints} \end{aligned} \qquad (71)$$

447 ## 3. Results and discussion

448 ### 3.1. Syngas synthesis under a single syngas technology

449 We optimized the superstructure for combinations of values of the parameters H_2/CO (1.0,
450 1.5, 2.0, 2.5) and P (1.0, 10, 20, 30 bar). The product syngas CO molar flow is fixed at 0.3
451 kmol/s and the CO_2/CO ratio is limited to 0.05. Since the quantity of syngas product is similar
452 and known between problems, we used Aspen HYSYS v8.4 to estimate molar flows and energy
453 consumptions. The variables are bounded according to these estimations. Upper bounds are
454 approximately five times higher than the calculated values. These estimated values are also
455 used to initialize the problem. The model consists in 467 equations and 357 variables, 24 of
456 which are binary variables. We used GAMS [36] to implement the model and solved it using
457 the ANTIGONE solver [37].

458 The resulting specific TAC (STAC) ($/kg syngas) and GWP (kg CO_2-eq/kg syngas) can be seen in
459 Figure 5. In this case, the maximum number of chosen syngas synthesis technologies to solve
460 the superstructure is fixed to one.

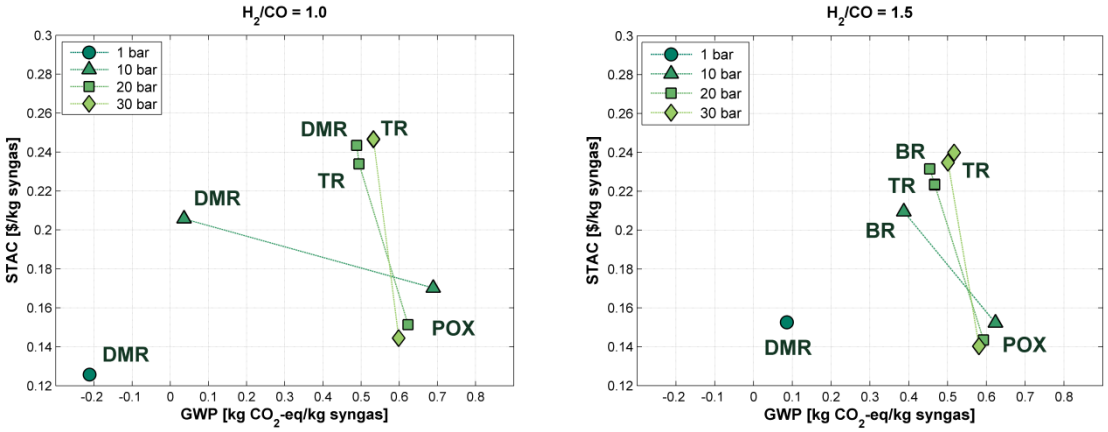

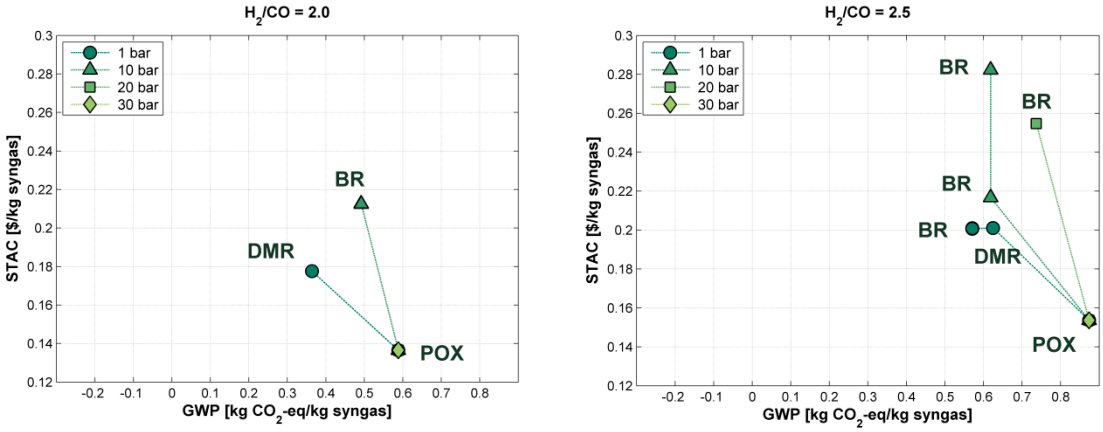

Figure 5.STAC-GWP Pareto set of solutions for syngas synthesis varying the product H_2/CO ratio and pressure for a single syngas synthesis process.

Most of the Pareto set of solutions consist in two points (minimum STAC – maximum GWP and vice versa) due to the system being unable to find an intermediate solution configuration. In some cases, the solution consists in only one point since that particular configuration achieves both minimum STAC and GWP for the desired syngas specifications. This condition is met when aiming for a H_2/CO ratio of 1.0 - 1.5 with a product pressure of 1 bar. As Figure 5 shows, DMR is single-handedly able to achieve the desired composition at these requirements with the aid of a WGS reactor (Appendix A1). The importance of this result resides in the fact that at a product pressure of 1 bar, the GWP indicator adopts a negative value of approximately -0.2 kg CO_2-eq/kg syngas, which means that the CO_2 consumption is greater than the indirect emission of the resources employed in the synthesis. As the required pressure rises, the optimal STAC and optimal GWP points split into two different configurations. The minimum STAC is achieved by employing the POX technology and is maintained as the lower STAC option across the remaining H_2/CO ratios and pressures. As can be seen in Table 5 and Figure A.4, in the POX technology and after heat integration, hot utilities are not required since raw materials can be preheated with the heat released in the reformer reactor due to the high exothermicity of the reforming reaction. This property makes POX a remarkable process cost-wise. In addition, for the cases where the H_2/CO ratio is 2.0 and pressure is 20-30 bar, and H_2/CO = 2.5 and P = 30 bar, both the minimum STAC and the minimum GWP configuration overlap and are led by the POX synthesis process. Regarding the minimum GWP extreme point, DMR, BR and TR (all three CO_2 consuming technologies) achieve the optimal values. The first appears when low pressure is required, the last at lower H_2/CO ratios and higher pressures, and the remaining one is the way to go at higher H_2/CO ratios, while still being used at ratios of 1.5.

The difference between STAC and GWP extreme solutions is the highest at a H_2/CO ratio of one and a pressure of 10 bar, where an increase of approximately 20 % in STAC achieves an outstanding decrease of almost 95 % in GWP from a maximum value of 0.7 kg CO_2-eq/kg syngas. On a second note, at a ratio of two and the same pressure, a reduction of 38 % in GWP while increasing the STAC a 22 % is achieved. Other cases apart from the previously mentioned only achieve a slight decrease of the GWP while notably increasing the STAC.

3.2. Syngas synthesis using a combination of syngas technologies

In order to test a potential synergistic combination of syngas processes, the optimizations were repeated allowing a maximum of two syngas synthesis technologies and maintaining the rest of conditions stablished in section 3.1. The results are given in Figure 6. The tendencies from Figure 5 persist while the number of Pareto points for a given pressure and ratio increase, as combinations of syngas technologies can reach lower GWP configurations than single technology systems. While minimizing the emission, at H_2/CO ratios of 1.0 and 1.5, the combination of DMR and BR— both CO_2 consuming processes— possesses the lowest GWP achievable by all these curves. As the STAC decreases— and the GWP rises— the resulting associations contain at least one CO_2 consuming process, being DMR the most used (in conjunction with SMR, POX or TR) followed by TR (along with BR or POX). When the H_2/CO ratio is between 2.0 and 2.5, the minimum GWP configuration for all the corresponding Pareto sets presents BR and SMR, due to BR managing to consume CO_2 but producing a H_2/CO ratio bellow two and SMR providing a high H_2/CO ratio to compensate. For all the curves, moving in the increasing GWP and decreasing STAC direction, CO_2 consuming processes can be found, such as DMR (only when P = 1 bar) with SMR, POX or CR; TR with SMR (ratio of 2.0 and P = 20 bar) and especially BR, combined with SMR, ATR, CR or POX. An exception for this trend is found at H_2/CO = 2.5 and P = 20 and 30 bar. In the first pair, only a single configuration with POX is used for all the solutions, while the second presents a SMR + POX non-CO_2 consuming association for all the intermediate points between the extreme solutions. Finally, for the minimum STAC extremes points, all Pareto sets except for the ones at 1 bar and 1.0 -1.5 H_2/CO ratios present POX configuration.

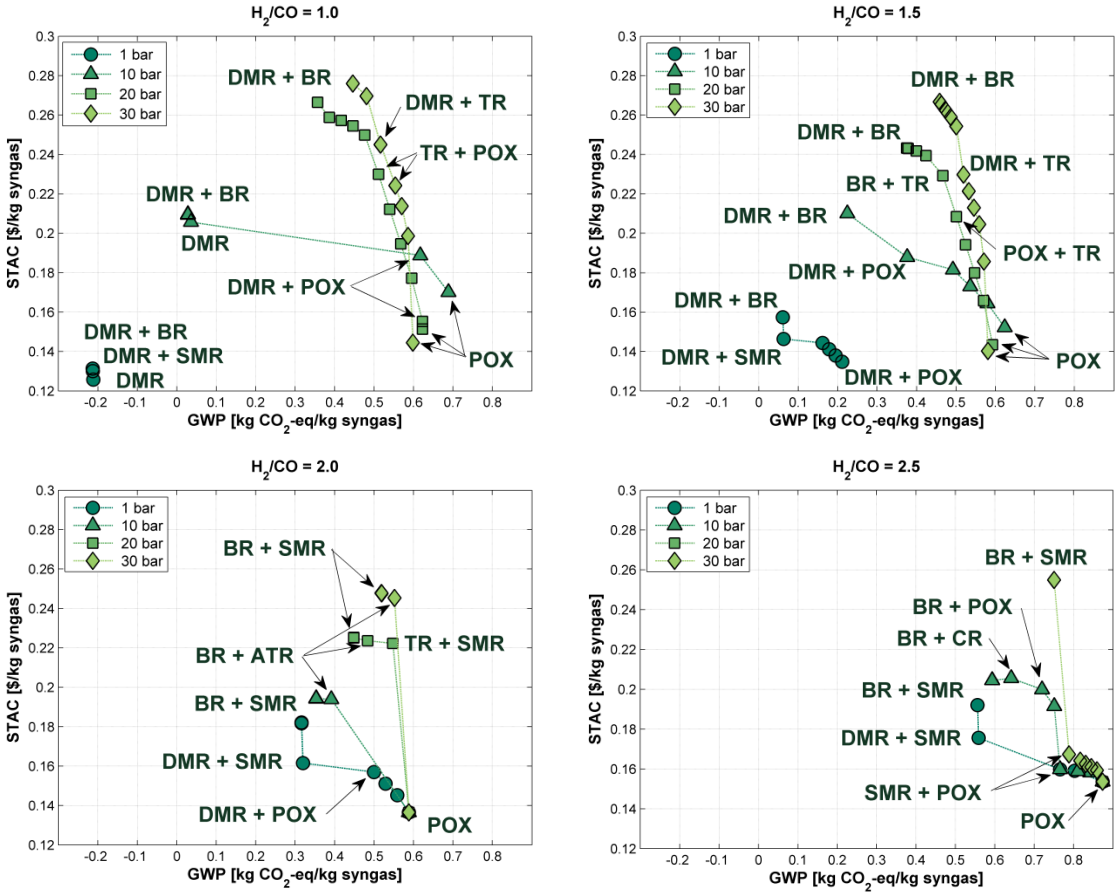

514 Figure 6.STAC-GWP Pareto set of solutions for syngas synthesis varying the product H_2/CO
515 ratio and pressure for the simultaneous utilization of two or less syngas synthesis processes.
516 Unlabeled points share the same technology combination as their closest nearside labeled
517 point that belongs to the same curve.

518 3.3. Effect of the CO_2/CO ratio

519 The inclusion of CO_2 in the syngas product gains interest in processes like methanol of Fischer-
520 Tropsch fuels synthesis, which under specific conditions and/or catalysts manage to consume it
521 in their main reactions. When this situation is met, the ratio of interest becomes $M = (H_2 - CO_2)$
522 / $(CO + CO_2)$, and for the mentioned processes takes a value around two. Hence, for this study
523 M is fixed at two, while varying the CO_2/CO ratio (0.05, 0.10, 0.15, 0.20, 0.30, 0.50) at a set
524 pressure of 30 bar of the product syngas. The variation in STAC and GWP of the optimized
525 syngas synthesis process can be seen in Figure 7.

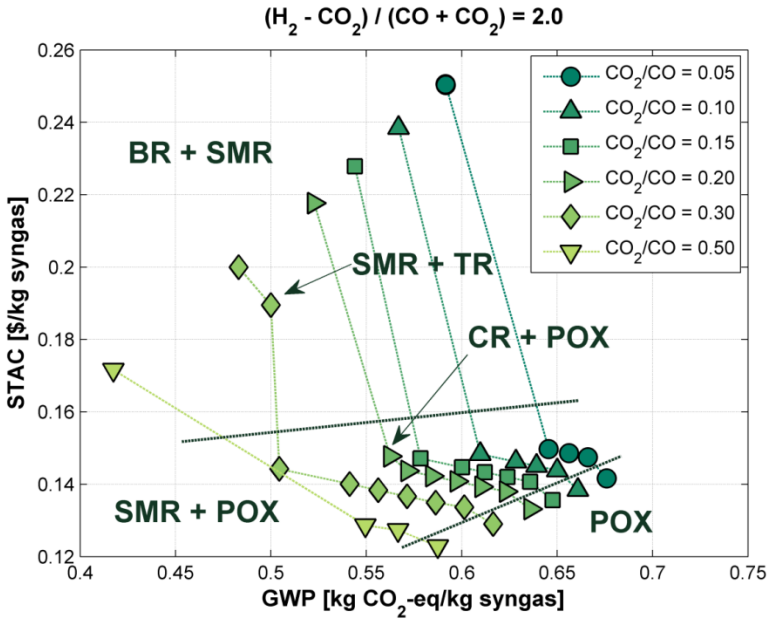

Figure 7. Pareto STAC-GWP curves at different CO_2/CO ratios for a fixed product syngas pressure of 30 bar and a value of two of the (H_2 - CO_2) / (CO + CO_2) ratio with at most two-syngas process combination.

In Figure 6, for the combination of 30 bar and a H_2/CO ratio of two, the processes used for the minimum emission configuration are BR and SMR, which after a drastic decrease in STAC, shift to SMR and POX. Finally, the minimum cost configuration is provided by POX. Two exclusive combinations appear for ratios of 0.20 and 0.30, showcasing CR and POX for the first ratio and SMR and TR for the second. The tendency is clear: increasing the CO_2/CO ratio decreases both the STAC and GWP of a given syngas. Regarding the STAC-GWP trade-off, at low CO_2/CO ratios, the difference in STAC when using CO_2 consuming processes is high, while the net GWP itself is practically invariable. However, for a CO_2/CO ratio of 0.50, the increase in cost (30 %) and decrease in emission (31 %) could be worth a more detailed study. In Figure 8, the consumed CO_2, defined as the CO_2 flow entering the superstructure minus the CO_2 flow leaving it by other means than the product, is plotted versus the GWP indicator. The figure shows that the minimum GWP points for all CO_2/CO ratios have similar CO_2 consumption, although it slightly decreases while this ratio increases. The consumption then suffers a sudden decrease even though the GWP indicator barely varies. This change addresses the importance of raw material and utility demands attached to each syngas process technology. Endothermic technologies, such as DMR, SMR or BR have high energy demands, which implies high cost and emission associated to them. However, the CO_2 consuming processes (DMR, BR) see their net GWP indicator reduced due to this consumption. This reduction is such that even after combining with an additional endothermic non CO_2-consuming process (SMR) the association is capable

of achieving the lowest GWP value in the studied conditions. This is why, when increasing the GWP indicator (associated to a STAC reduction (Figure 7)), one of the processes (BR) shifts to a low energy demand technology (POX)— which does not consume CO_2— to achieve lower costs (and emissions) due to the reduced energy usage. Nevertheless, even though the energy demand has been decreased, the net GWP value is higher due to the lack of CO_2 reutilization. Finally, for the minimum extreme points of maximum GWP configurations, consumption adopts negative values, indicating that there is no reutilization of CO_2 at all, or at least the production of the gas surpasses its consumption.

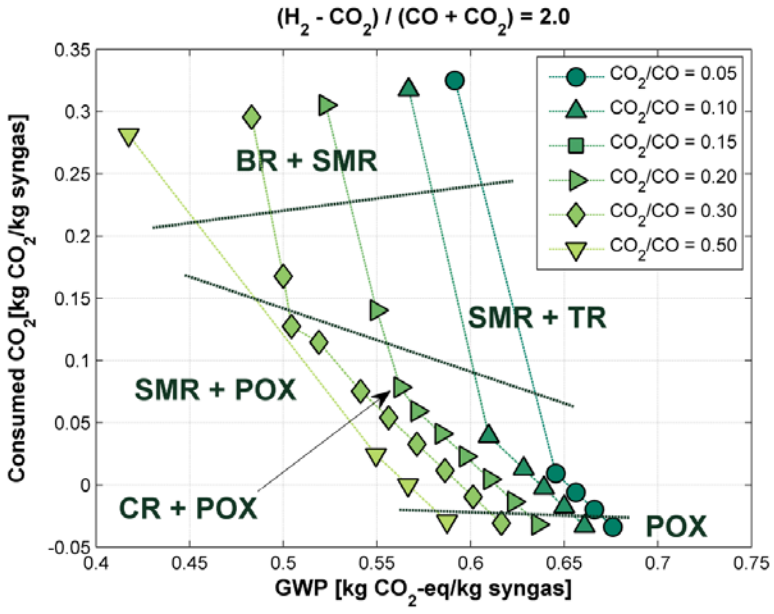

Figure 8.Effect of the consumption of CO_2 versus on the net GWP per kg of synthesized syngas at a $(H_2 - CO_2) / (CO + CO_2)$ ratio of two, product pressure of 30 bar and variable CO_2/CO ratio with a two-syngas process combination.

4. Conclusions

Syngas is a mixture of H_2, CO and CO_2. The mixture is of great importance in the synthesis of synthetic fuels and other chemicals. The diversity of its production paths and product specifications required for its different uses makes syngas an interesting case of study, especially since CO_2 can be utilized in the synthesis. In this work, we propose a superstructure containing a variety of syngas process technologies and auxiliary units in order to produce and adjust syngas to several composition and pressure specifications. The results show that at low H_2/CO ratios and pressures, dry methane reforming (DMR) can net consume CO_2. By contrast, all the cases indicate that POX minimizes the STAC. When allowing up to two different syngas processes to operate simultaneously, the lowest emission configurations are achieved by DMR + BR for a H_2/CO ratio between 1.0 and 1.5, and BR + SMR for H_2/CO ratios between 2.0 and 2.5. However, the minimum cost configurations are still achieved by using POX.

When setting a (H_2 - CO_2) / (CO + CO_2) ratio to two, the increase of the CO_2/CO ratio in the syngas shows a decrease of cost and emission. At the maximum GWP (minimum cost) configurations, CO_2 is emitted with a value of 0.03 - 0.04 kg CO_2/kg syngas. However, a significant increase in the CO_2 consumption is achieved with only a slight penalization in the cost. In addition, the results show that a maximum of 0.3 kg CO_2 per kg of syngas produced can be obtained with the synergistic combination of BR and SMR technologies.

5. Acknowledgements

The authors gratefully acknowledge financial support to the Spanish «Ministerio de Economía, Industria y Competitividad» under project CTQ2016-77968-C3-2-P (AEI/FEDER, UE).

6. References

1. European Comission, J.R.C. *EDGAR - Emission Database for Global Atmospheric Research*. 2015 March 2016]; Available from: http://edgar.jrc.ec.europa.eu/overview.php?v=CO2ts1990-2014.
2. Leung, D.Y.C., G. Caramanna, and M.M. Maroto-Valer, *An overview of current status of carbon dioxide capture and storage technologies.* Renewable and Sustainable Energy Reviews, 2014. **39**(0): p. 426-443.
3. Ke Liu, C.S., Velu Subramani, *Hydrogen and Syngas Production and Purification Technologies*. 2010: Wiley.
4. Reyes, S.C., J.H. Sinfelt, and J.S. Feeley, *Evolution of Processes for Synthesis Gas Production: Recent Developments in an Old Technology.* Industrial & Engineering Chemistry Research, 2003. **42**(8): p. 1588-1597.
5. *Haldor Topsoe* [cited 2017 September 8th]; Available from: https://www.topsoe.com/products/autothermal-reformer-atr.
6. *Sasol Technology* [cited 2017 September 8th]; Available from: http://www.sasol.com/sites/sasol/files/presentations_speeches/Recent%20Advances%20in%20Sasol%E2%80%99s%20GTL%20Technology%20%E2%80%93%20January%202013.pdf.
7. Trevisanut, C., et al., *Micro-syngas technology options for GtL*. Vol. 94. 2016. n/a-n/a.
8. *Air Liquid Engineering & Construction* [cited 2017 September 8th]; Available from: https://www.engineering-airliquide.com/autothermal-reforming-atr-syngas-generation.
9. *John Matthey Process Technologies* [cited 2017 September 8th]; Available from: http://www.jmprotech.com/core-technologies-reforming-ATR-GHR-SMR.
10. Font Freide, J.J.H.M., et al., *An Adventure in Catalysis: The Story of the BP Fischer–Tropsch Catalyst from Laboratory to Full-Scale Demonstration in Alaska.* Topics in Catalysis, 2003. **26**(1): p. 3-12.
11. *The Linde Group* [cited 2017 September 8th]; Available from: http://www.linde-engineering.com/en/process_plants/hydrogen_and_synthesis_gas_plants/gas_generation/partial_oxidation/index.html.
12. *The Linde Group* [cited 2017 September 12th]; Available from: https://www.hzg.de/imperia/md/content/gkss/institut_fuer_werkstoffforschung/wtn/h2-speicher/funchy/funchy-2007/5_linde_wawrzinek_funchy-2007.pdf.
13. *Haldor-Topsoe* [cited 2017 September 12th]; Available from: https://www.topsoe.com/sites/default/files/topsoe_large_scale_hydrogen_produc.pdf.
14. *Ullmann's Encyclopedia of Industrial Chemistry*. 6th ed. 2002: Wiley - VCH.

15. Lim, Y., et al., *Optimal design and decision for combined steam reforming process with dry methane reforming to reuse CO_2 as a raw material.* Industrial and Engineering Chemistry Research, 2012. **51**(13): p. 4982-4989.
16. Farniaei, M., et al., *Simultaneous production of two types of synthesis gas by steam and tri-reforming of methane using an integrated thermally coupled reactor: Mathematical modeling.* International Journal of Energy Research, 2014. **38**(10): p. 1260-1277.
17. Farniaei, M., et al., *Syngas production in a novel methane dry reformer by utilizing of tri-reforming process for energy supplying: Modeling and simulation.* Journal of Natural Gas Science and Engineering, 2014. **20**(0): p. 132-146.
18. Richard Turton, R.C.B., Wallace B. Whiting, Joseph A. Shaeiwitz, Debangsu Bhattacharyya, *Analysis, Synthesis and Design of Chemical Processes*. Fourth Edition ed. 2012: Prentice Hall.
19. Peña, M.A., J.P. Gómez, and J.L.G. Fierro, *New catalytic routes for syngas and hydrogen production.* Applied Catalysis A: General, 1996. **144**(1–2): p. 7-57.
20. Bobrova, L.N., et al., *Kinetic assessment of dry reforming of methane on Pt+Ni containing composite of fluorite-like structure.* Applied Catalysis B: Environmental, 2016. **182**: p. 513-524.
21. Julián-Durán, L.M., et al., *Techno-economic assessment and environmental impact of shale gas alternatives to methanol.* ACS Sustainable Chemistry and Engineering, 2014. **2**(10): p. 2338-2344.
22. Lange, J.-P., *Methanol synthesis: a short review of technology improvements.* Catalysis Today, 2001. **64**(1–2): p. 3-8.
23. Raju, A.S.K., C.S. Park, and J.M. Norbeck, *Synthesis gas production using steam hydrogasification and steam reforming.* Fuel Processing Technology, 2009. **90**(2): p. 330-336.
24. Zahedi nezhad, M., S. Rowshanzamir, and M.H. Eikani, *Autothermal reforming of methane to synthesis gas: Modeling and simulation.* International Journal of Hydrogen Energy, 2009. **34**(3): p. 1292-1300.
25. Olah, G.A., et al., *Bi-reforming of methane from any source with steam and carbon dioxide exclusively to metgas (CO-2H_2) for methanol and hydrocarbon synthesis.* Journal of the American Chemical Society, 2013. **135**(2): p. 648-650.
26. Frischknecht, R., et al., *The ecoinvent Database: Overview and Methodological Framework (7 pp).* The International Journal of Life Cycle Assessment, 2005. **10**(1): p. 3-9.
27. Yee, T.F. and I.E. Grossmann, *Simultaneous optimization models for heat integration—II. Heat exchanger network synthesis.* Computers & Chemical Engineering, 1990. **14**(10): p. 1165-1184.
28. *Ecoinvent Database 3.3*. 2017; Available from: http://www.ecoinvent.org/.
29. Nuchitprasittichai, A. and S. Cremaschi, *Optimization of CO_2 capture process with aqueous amines using response surface methodology.* Computers & Chemical Engineering, 2011. **35**(8): p. 1521-1531.
30. Chiang, Y.C. and C.T. Chang, *Single-objective and multiobjective designs for hydrogen networks with fuel cells.* Industrial and Engineering Chemistry Research, 2014. **53**(14): p. 6006-6020.
31. Wu, B., et al., *Assessment of the energy consumption of the biogas upgrading process with pressure swing adsorption using novel adsorbents.* Journal of Cleaner Production, 2015. **101**: p. 251-261.
32. Ribeiro, A.M., J.C. Santos, and A.E. Rodrigues, *PSA design for stoichiometric adjustment of bio-syngas for methanol production and co-capture of carbon dioxide.* Chemical Engineering Journal, 2010. **163**(3): p. 355-363.

33. Smith R J, B., M. Loganathan, and M.S. Shantha, *A review of the water gas shift reaction kinetics.* International Journal of Chemical Reactor Engineering, 2010. **8**.
34. Lee, S. and I.E. Grossmann, *New algorithms for nonlinear generalized disjunctive programming.* Computers & Chemical Engineering, 2000. **24**(9–10): p. 2125-2141.
35. Ehrgott, M. and M.M. Wiecek, *Multiobjective programming*, in *International Series in Operations Research and Management Science*. 2005. p. 667-722.
36. *GAMS Development Corporation. General Algebraic Modeling System (GAMS) Release 24.8.1. Washington, DC, USA, 2016*.
37. Misener, R. and C.A. Floudas, *ANTIGONE: Algorithms for coNTinuous / Integer Global Optimization of Nonlinear Equations.* Journal of Global Optimization, 2014. **59**(2): p. 503-526.

APPENDIX A

- **Syngas processes before and after heat integration.**

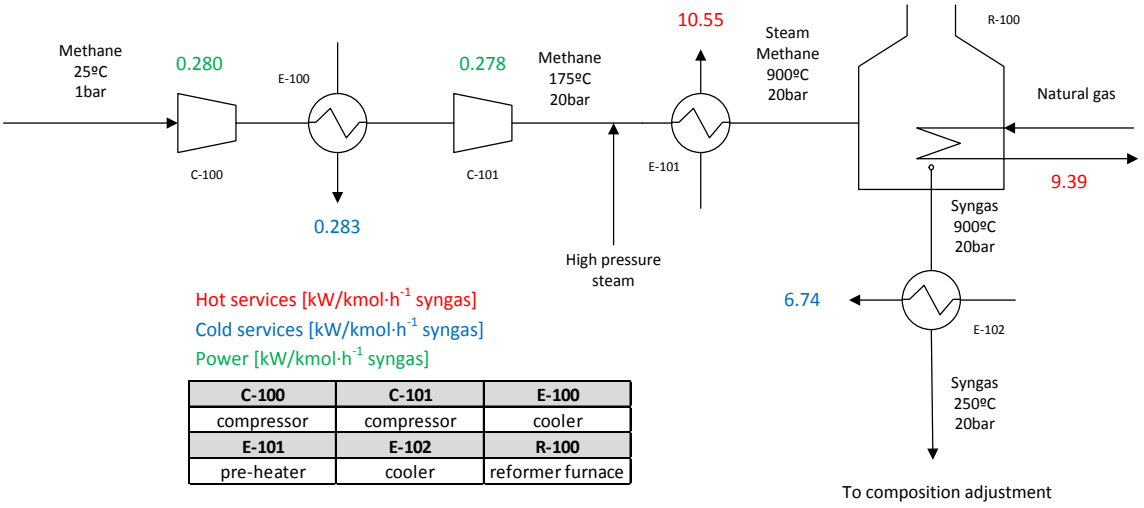

C-100	C-101	E-100
compressor	compressor	cooler
E-101	**E-102**	**R-100**
pre-heater	cooler	reformer furnace

Figure A. 1. Proposed steam methane reforming (SMR) basic process.

C-100	C-101	E-100	E-101	E-102	E-103	R-100
compressor	compressor	cooler	pre-heater	pre-heater	cooler	reformer furnace

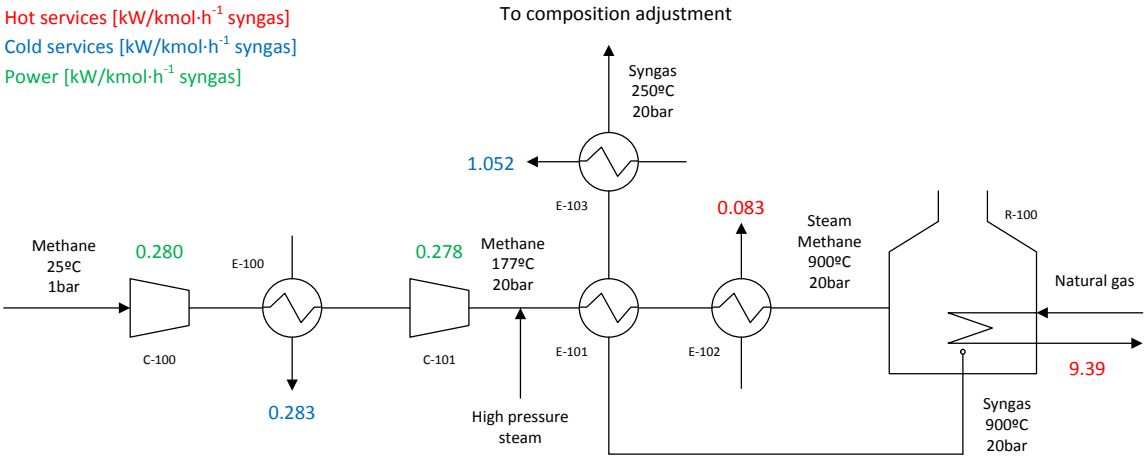

690
691

692 Figure A. 2. Proposed steam methane reforming (SMR) process after heat integration.

C-100	C-101	C-102	C-103	E-100
compressor	compressor	compressor	compressor	cooler
E-101	**E-102**	**E-103**	**R-100**	
cooler	pre-heater	cooler	reformer furnace	

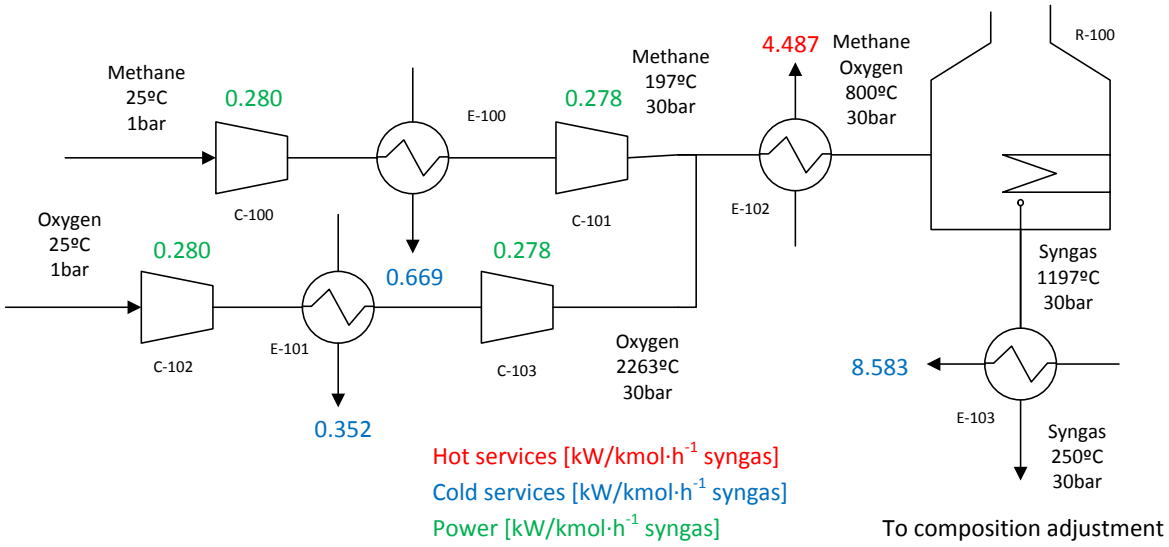

693
694

695 Figure A. 3. Proposed partial oxidation (POX) basic process.

696

C-100	C-101	C-102
compressor	compressor	compressor
C-103	**E-100**	**E-101**
compressor	cooler	cooler
E-102	**E-103**	**R-100**
pre-heater	cooler	reformer furnace

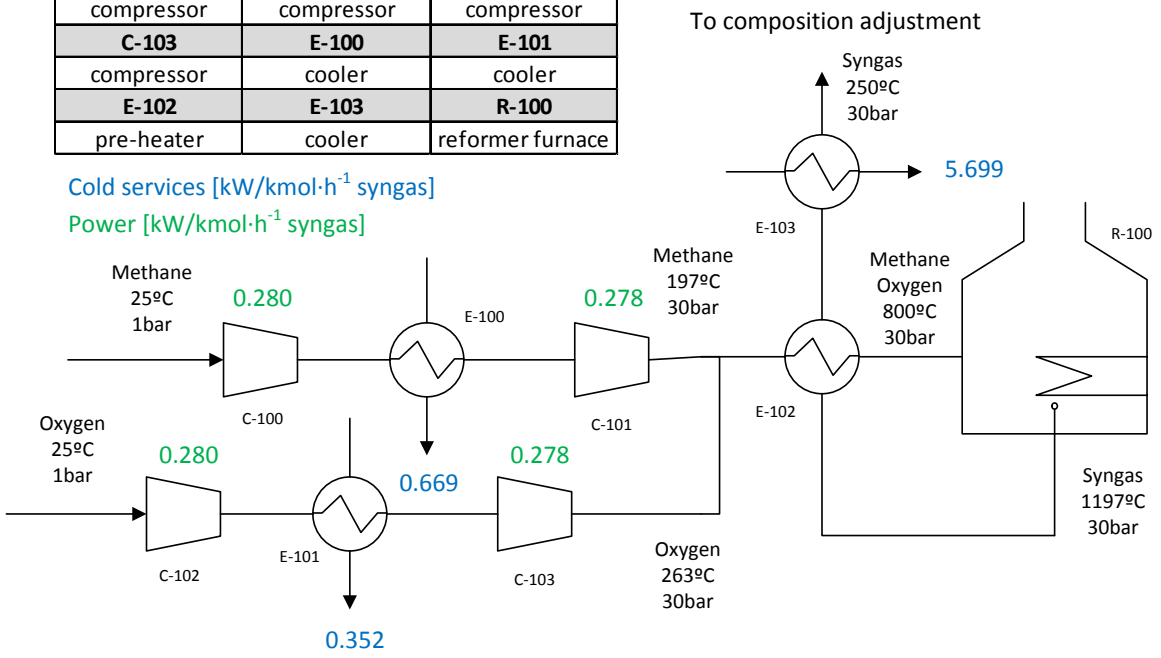

Figure A.1. Proposed partial oxidation (POX) process after heat integration.

C-100	C-101	C-102	C-103	E-100
compressor	compressor	compressor	compressor	cooler
E-101	**E-102**	**E-103**	**R-100**	
cooler	pre-heater	cooler	reformer furnace	

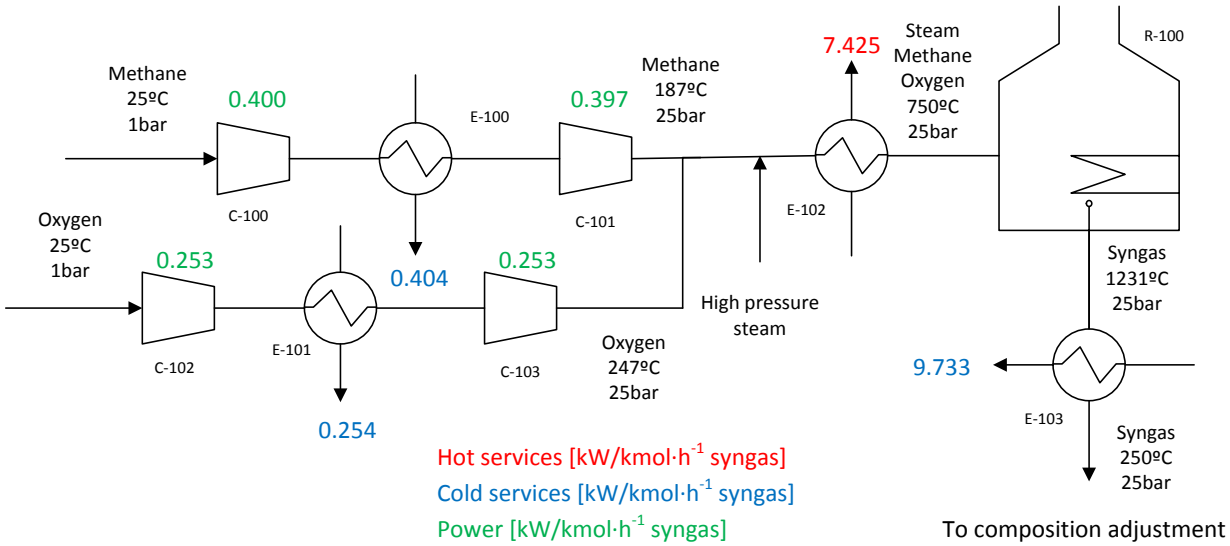

Figure A.2. Proposed auto-thermal reforming (ATR) basic process.

C-100	C-101	C-102
compressor	compressor	compressor
C-103	**E-100**	**E-101**
compressor	cooler	cooler
E-102	**E-103**	**R-100**
pre-heater	cooler	reformer furnace

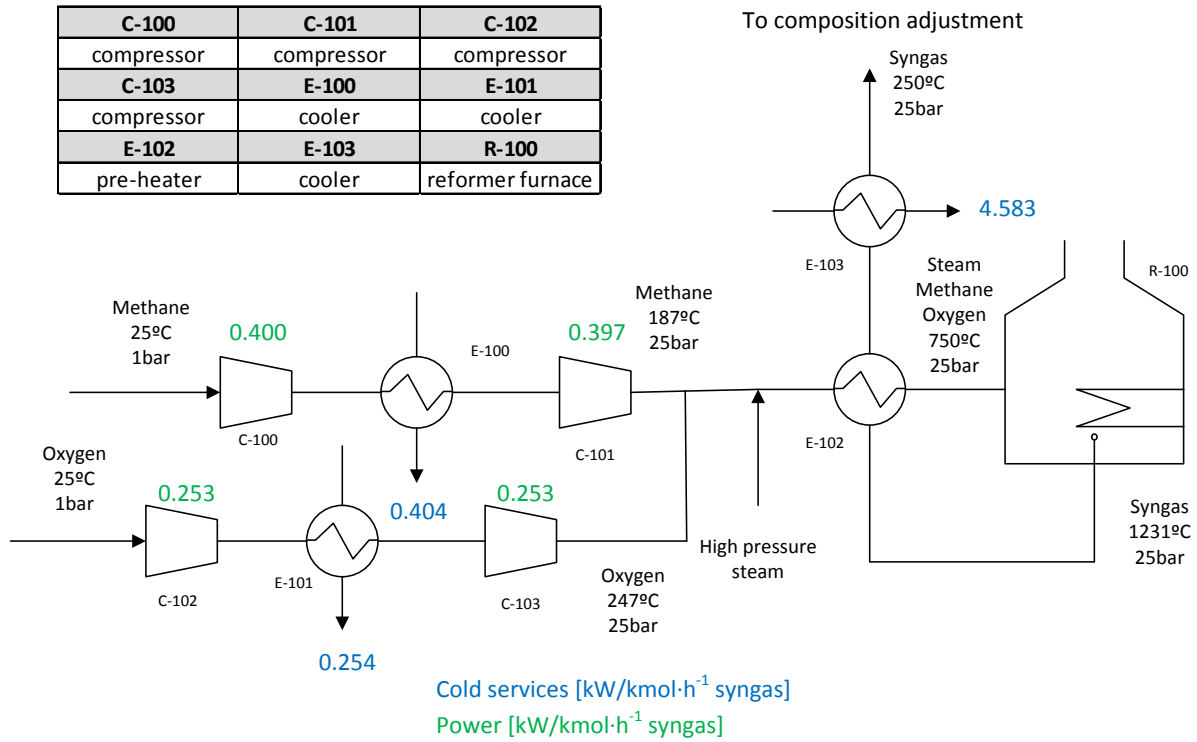

Figure A.3. Proposed auto-thermal reforming (ATR) process after heat integration.

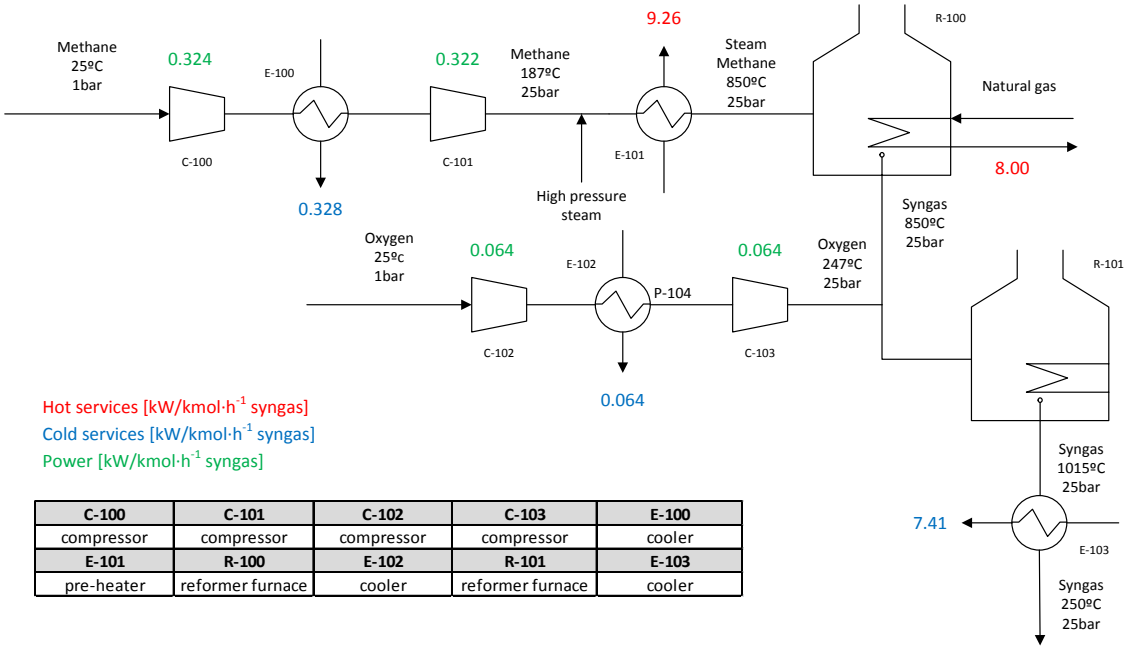

C-100	C-101	C-102	C-103	E-100
compressor	compressor	compressor	compressor	cooler
E-101	**R-100**	**E-102**	**R-101**	**E-103**
pre-heater	reformer furnace	cooler	reformer furnace	cooler

Figure A.4. Proposed combined reforming (CR) basic process.

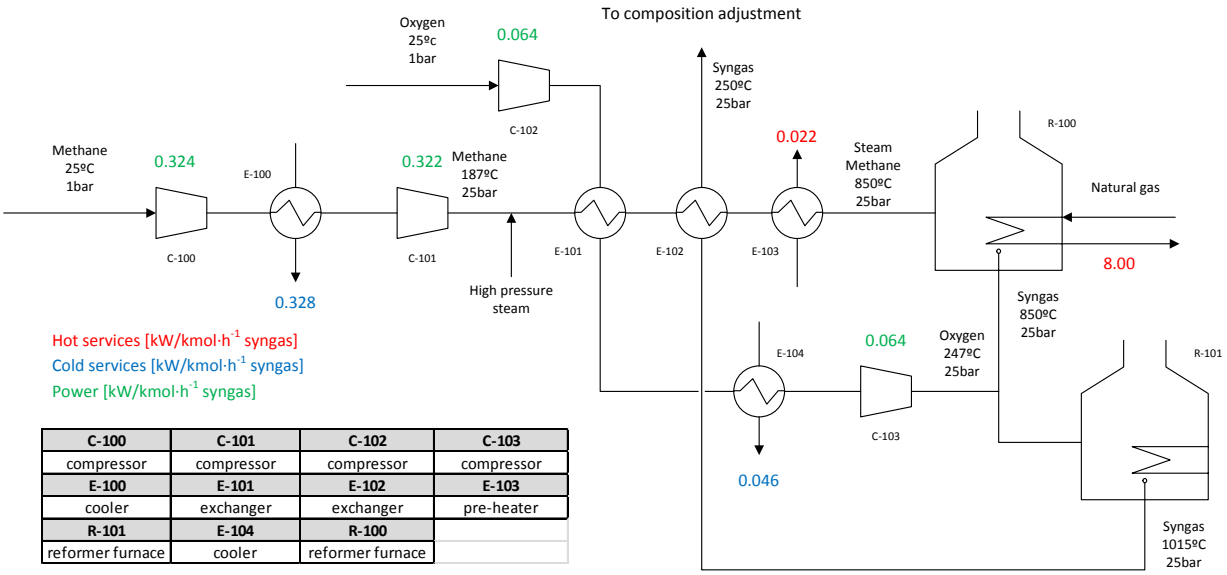

C-100	C-101	C-102	C-103
compressor	compressor	compressor	compressor
E-100	**E-101**	**E-102**	**E-103**
cooler	exchanger	exchanger	pre-heater
R-101	**E-104**	**R-100**	
reformer furnace	cooler	reformer furnace	

Figure A.5. Proposed combined reforming (CR) process after heat integration.

E-100	E-101	R-100
pre-heater	cooler	reformer furnace

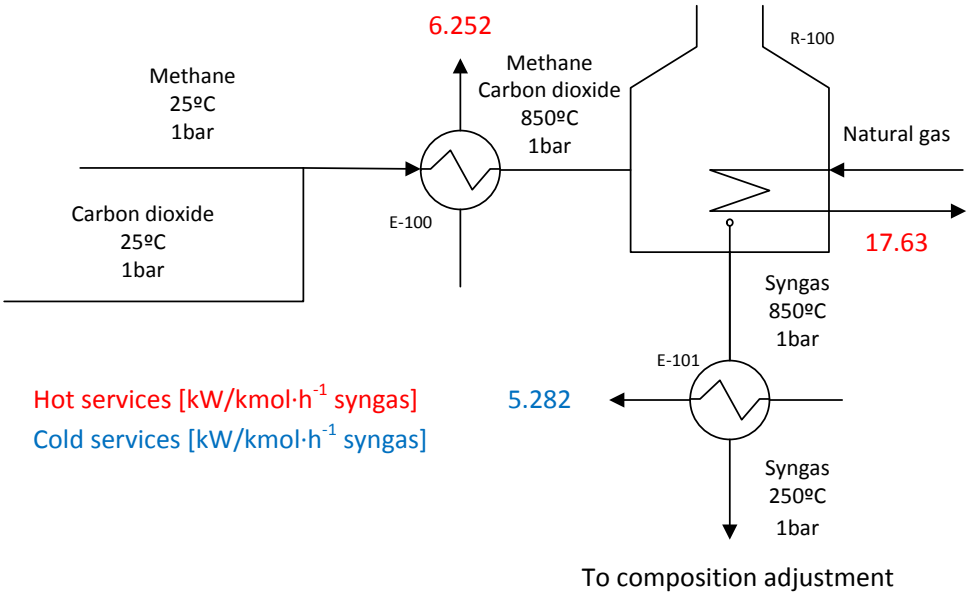

Figure A.6. Proposed dry methane reforming (DMR) basic process.

E-100	E-101	R-100
pre-heater / cooler	pre-heater	reformer furnace

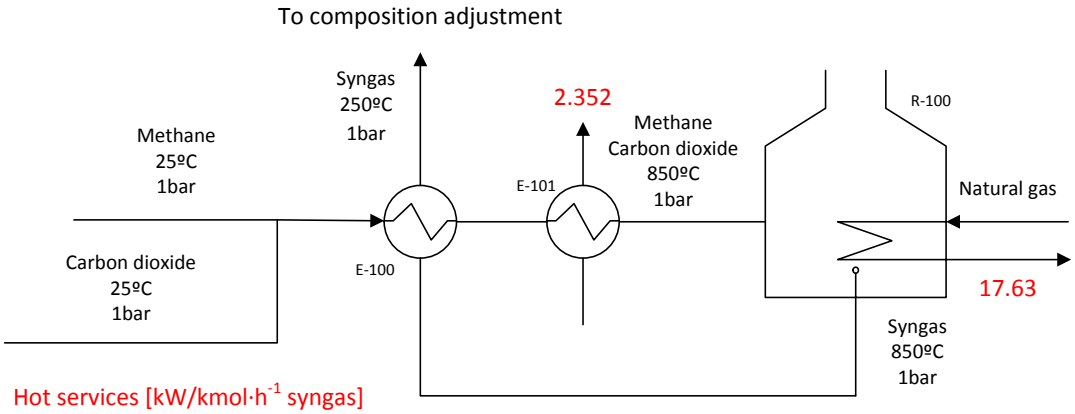

722

723 Figure A.7. Proposed dry methane reforming (DMR) after heat integration..

724

725

C-100	C-101	E-100	E-101	R-100
compressor	compressor	pre-heater	cooler	reformer furnace

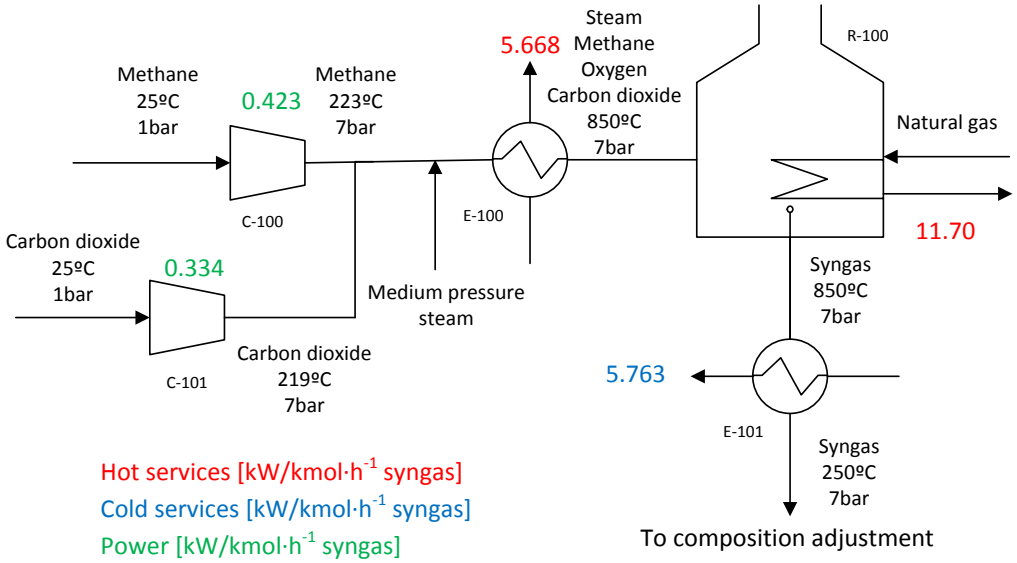

726

727 Figure A.8. Proposed bi-reforming (BR) basic process.

728

729

C-100	C-101	E-100	E-101	E-102	R-100
compressor	compressor	pre-heater	cooler	pre-heater	reformer furnace

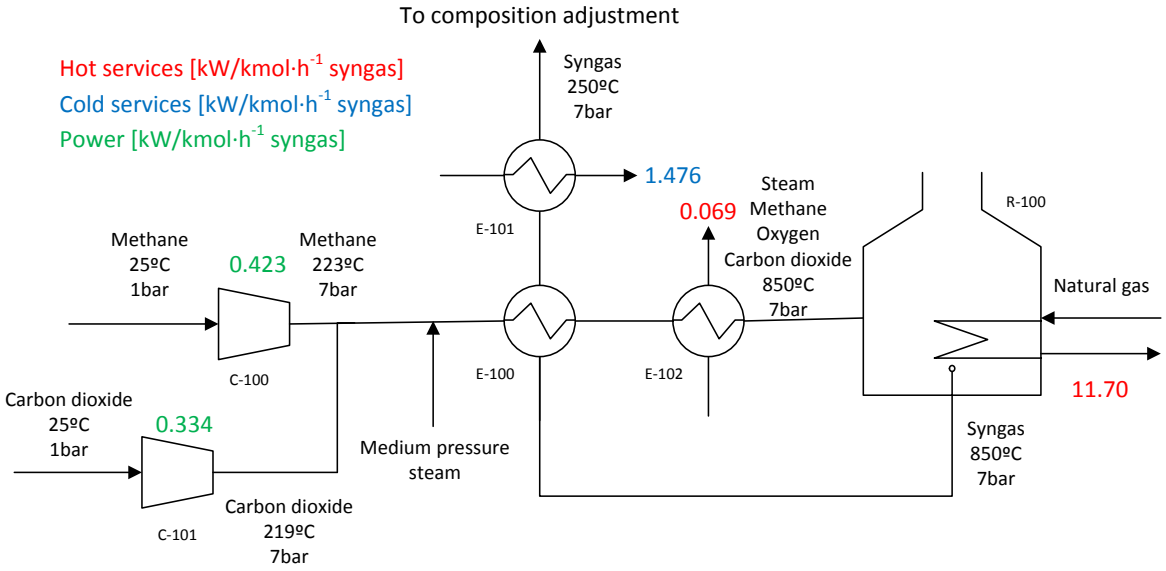

Figure A.9. Proposed bi-reforming (BR) process after heat integration.

C-100	C-101	C-102	C-103	C-104	C-105
compressor	compressor	compressor	compressor	compressor	compressor
E-100	**E-101**	**E-102**	**E-103**	**E-104**	**R-100**
cooler	cooler	cooler	pre-heater	pre-heater	reformer furnace

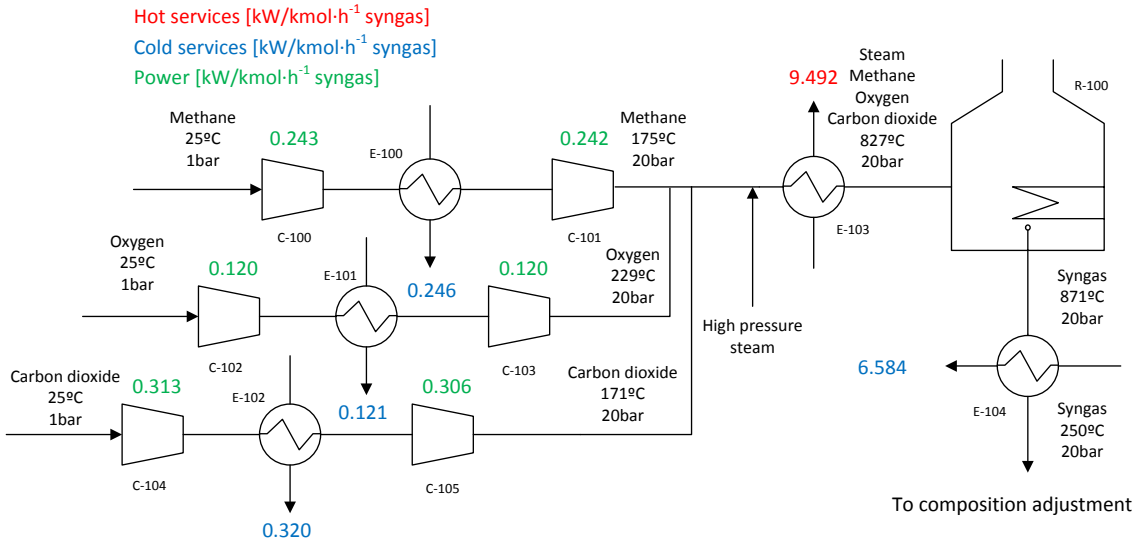

Figure A.10. Proposed tri-reforming (TR) basic process.

C-100	C-101	C-102	C-103	C-104	C-105	R-100
compressor	compressor	compressor	compressor	compressor	compressor	reformer furnace
E-100	**E-101**	**E-102**	**E-103**	**E-104**	**E-105**	
cooler	cooler	cooler	exchanger	exchanger	pre-heater	

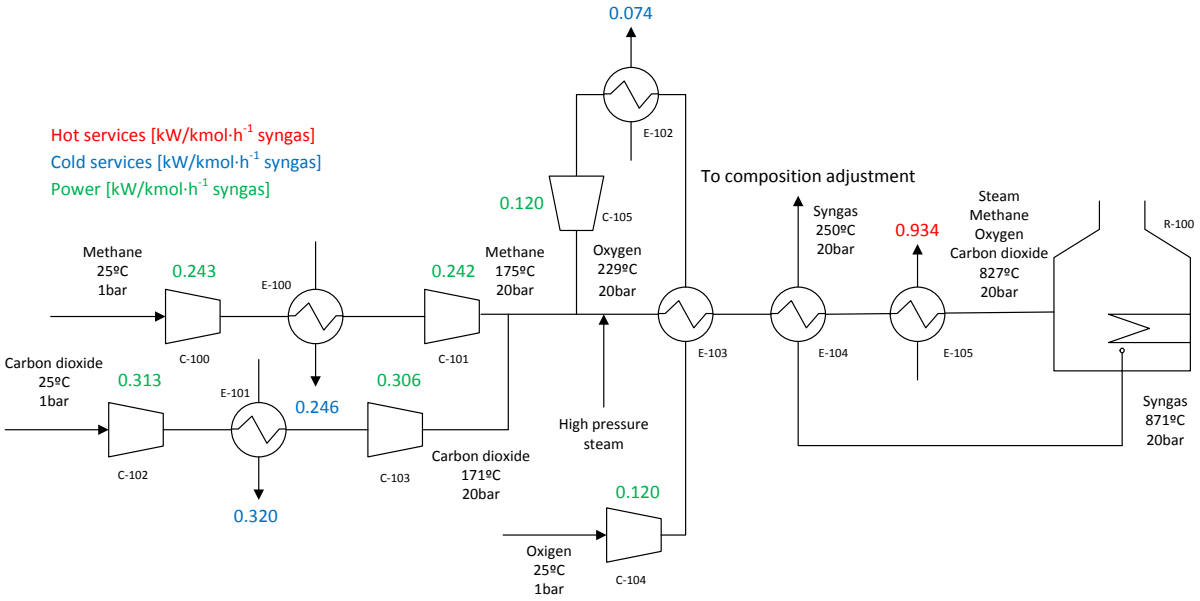

Figure A.11. Proposed tri-reforming (TR) process after heat integration.

APPENDIX B

- **Calculated parameters used in the optimization**

Table B.1. Values of χ_{ij} in kmol of component j exiting process i per kmol of fresh methane entering the process.

	Methane	Steam	O_2	CO_2	CO	H_2
SMR	0.0912	1.8028	0.0000	0.2882	0.6205	3.0144
POX	0.0711	0.0591	0.0000	0.0120	0.9168	1.7985
ATR	0.0007	1.4205	0.0000	0.2100	0.7892	2.0079
CR	0.0213	1.6501	0.0000	0.2463	0.7324	2.8069
DMR	0.0592	0.0305	0.0000	0.0287	1.9119	1.8508
BR	0.0735	1.0043	0.0000	0.4691	1.2572	2.4483
TR	0.0354	2.5248	0.0000	1.2103	1.0541	1.8640

Table B.2. Energetic demand of process i in kWh of utility u per kmol of fresh methane fed to the process.

	Power	Cooling water	Natural gas
SMR	3.245	7.767	55.11
POX	5.763	19.21	0.000

ATR	5.768	23.21	0.000
CR	4.229	2.047	43.78
DMR	0.000	0.000	77.54
BR	3.976	7.754	61.82
TR	8.989	0.521	6.245

749

750 Table B.3. Emission φ_{iu} in kg of CO_2-eq emitted of utility u per kmol of methane fed to process i.

	Power	**Cooling water**	**Natural gas**
SMR	1.991	0.000	33.82
POX	3.536	0.000	0.000
ATR	3.539	0.000	0.000
CR	2.595	0.000	26.87
DMR	0.000	0.000	47.58
BR	2.440	0.000	37.94
TR	5.516	0.000	3.83

751

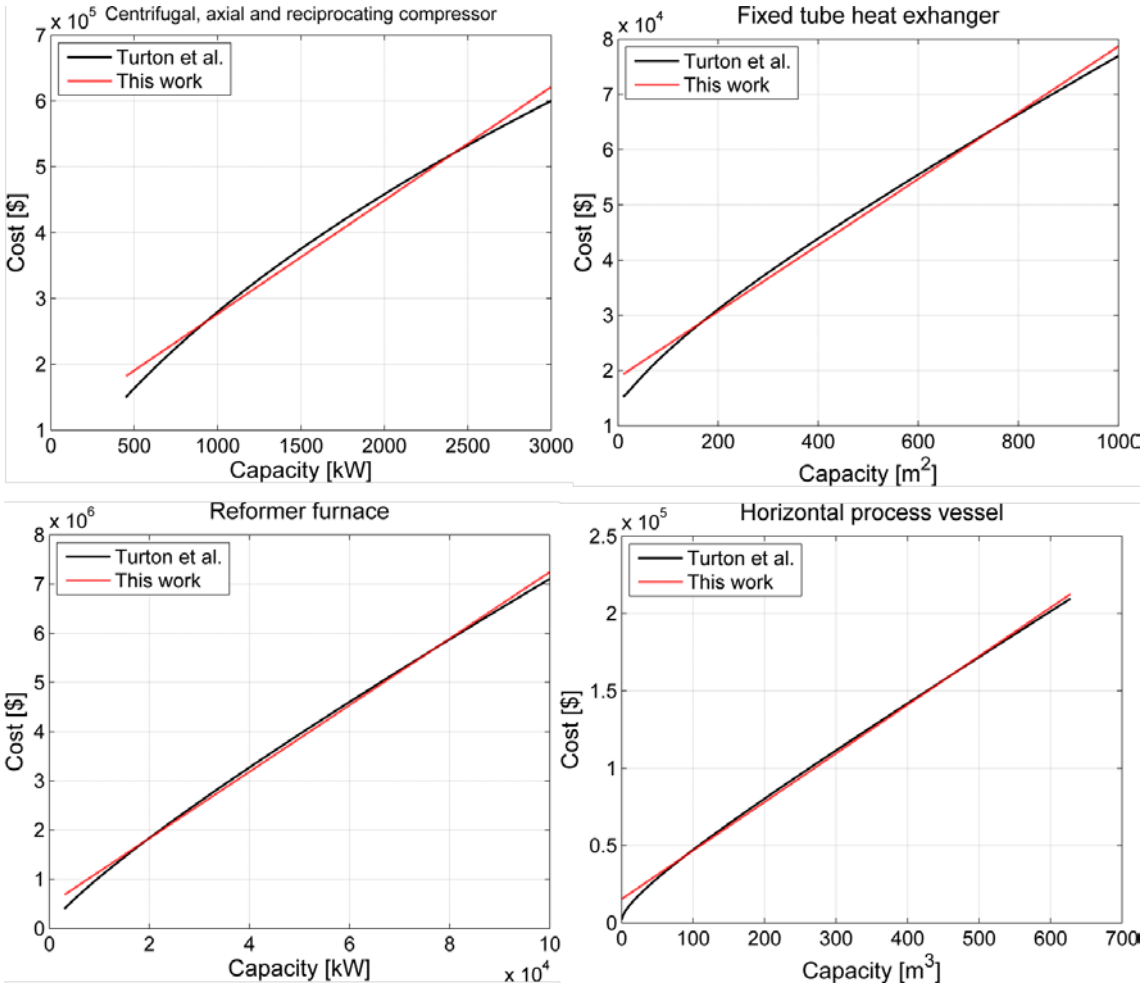

752

Figure B.1. Comparison among the original capital cost relations for compressors, heat exchangers, reformer furnaces and process vessels [18] and the work linearization used in this work.

Table B.4. Fixed C_{ik}^{f} and variable C_{ik}^{v} cost parameters of process units shown in Figure B.1.

Unit	C_{ik}^{f} ·10^{-4} [$]	C_{ik}^{v} [$/capacity units]
Compressor	10.43	172.4
Heat exchanger	1.871	59.99
Reformer furnace	48.01	67.64
Process vessel*	1.531	314.1

*used for absorber columns, flash separator and WGS reactor.

APPENDIX C

- **Relevant results of the multiobjective optimization of syngas synthesis**

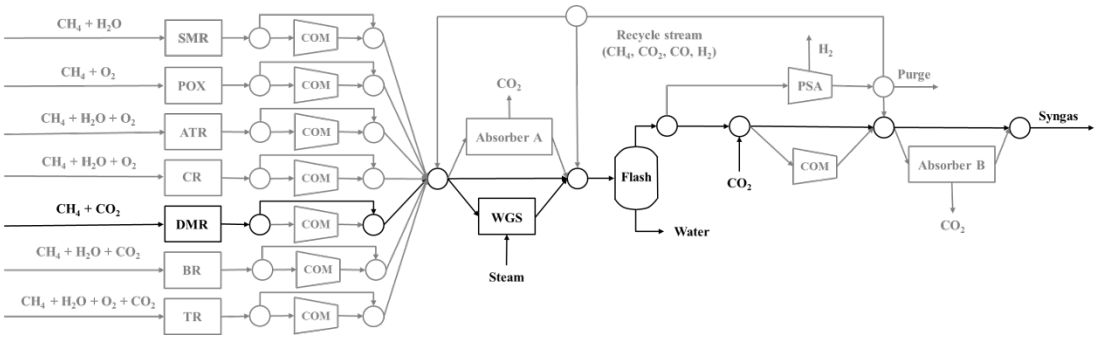

Figure C.9. Flow diagram result from the superstructure optimization for minimum emission for H_2/CO = 1.0 and P = 1.0 bar.

Table C.1. Molar flow results [kmol/s] of Figure C.9.

	DMR inlet	DMR outlet	WGS inlet	WGS outlet	Flash inlet	Flash outlet	Syngas Product
Methane	0.159	0.009	0.008	0.008	0.009	0.009	0.009
Water/Steam	-	0.005	0.004	0.000	0.000	-	-
Oxygen	-	-	-	-	-	-	-
Carbon dioxide	0.159	0.005	0.004	0.009	0.009	0.009	0.015
Carbon monoxide	-	0.305	0.274	0.270	0.300	0.300	0.300

Hydrogen	-	0.295	0.266	0.270	0.300	0.300	0.300

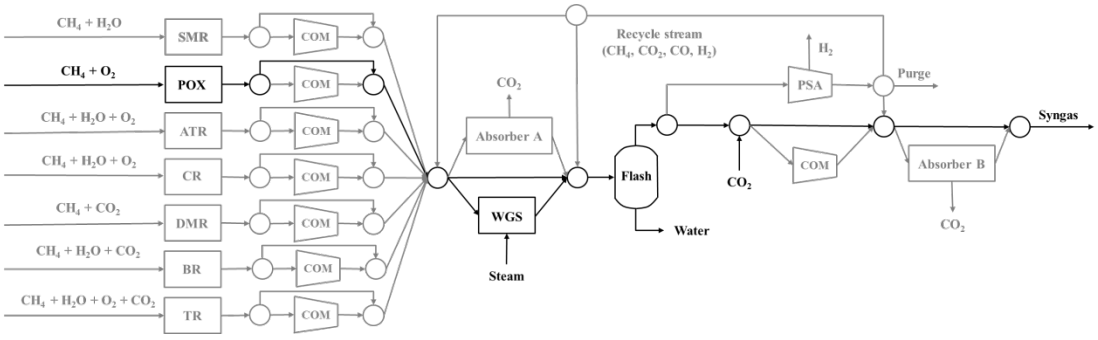

Figure C.10. Flow diagram result from the superstructure optimization for minimum cost for $H_2/CO = 2.0$ and P = 1.0, 10, 20 and 30 bar.

Table C. 2. Molar flow results [kmol/s] of Figure C.10.

	POX inlet	**POX outlet**	**WGS inlet**	**WGS outlet**	**Flash inlet**	**Flash outlet**	**Syngas Product**
Methane	0.331	0.024	0.005	0.005	0.024	0.024	0.024
Water/Steam	-	0.020	0.004	0.000	0.016	-	-
Oxygen	0.166	-					-
Carbon dioxide	-	0.004	0.001	0.005	0.008	0.008	0.015
Carbon monoxide	-	0.304	0.062	0.058	0.300	0.300	0.300
Hydrogen	-	0.596	0.122	0.126	0.600	0.600	0.600

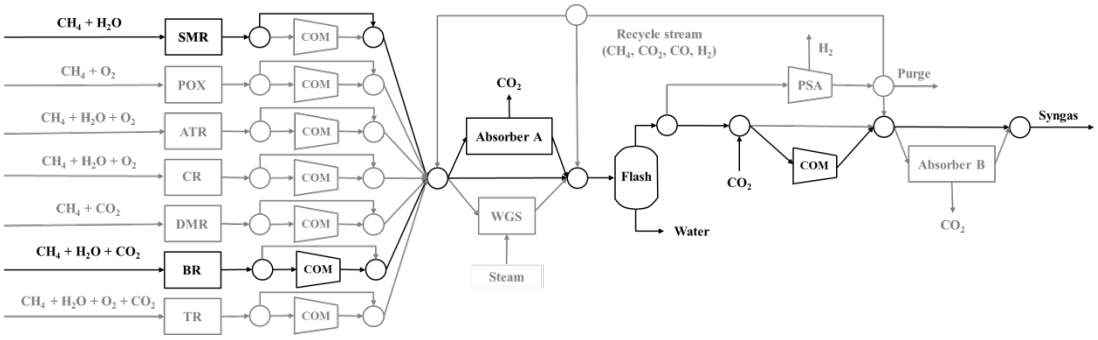

Figure C.11. Flow diagram result from the superstructure optimization for minimum emission for $(H_2-CO_2)/(CO+CO_2) = 2.0$, $CO_2/CO = 0.50$ and P = 30 bar.

784 Table C. 3. Molar flow results [kmol/s] of Figure C.11.

	SMR inlet	SMR outlet	BR inlet	BR outlet	Absorber inlet	Absorber outlet	Flash inlet	Flash outlet	Syngas Product
Methane	0.258	0.023	0.111	0.008	0.003	0.003	0.032	0.032	0.032
Water/Steam	0.774	0.465	0.178	0.112	0.058	0.058	0.577	-	-
Oxygen	-	-	-	-	-	-	-	-	-
Carbon dioxide	-	0.074	0.089	0.052	0.013	0.001	0.114	0.114	0.150
Carbon monoxide	-	0.160	-	0.140	0.030	0.030	0.300	0.300	0.300
Hydrogen	-	0.777	-	0.273	0.105	0.105	1.050	1.050	1.050

785

786